

1 **ARIOS: a database for ocean acidification assessment in the Iberian Upwelling**
2 **System (1976 - 2018).**

3
4 **Xosé Antonio Padin*¹, Antón Velo¹ and Fiz F. Pérez¹**

5 ¹ Instituto de Investigaciones Marinas, IIM-CSIC, 36208 Vigo, Spain.

6 padin@iim.csic.es, avelo@iim.csic.es, fiz.perez@iim.csic.es

7
8 **1. Abstract**

9 A data product of 17,653 discrete samples from 3,343 oceanographic stations
10 combining measurements of pH, alkalinity and other biogeochemical parameters off the
11 North-western Iberian Peninsula from June 1976 to September 2018 is presented in this
12 study. The oceanography cruises funded by 24 projects were primarily carried out in the
13 *Ría de Vigo* coastal inlet, but also in an area ranging from the Bay of Biscay to the
14 Portuguese coast. The robust seasonal cycles and long-term trends were only calculated
15 along a longitudinal section, gathering data from the coastal and oceanic zone of the
16 Iberian Upwelling System. The pH in the surface waters of these separated regions,
17 which were highly variable due to intense photosynthesis and the remineralization of
18 organic matter, showed an interannual acidification ranging from -0.0016 yr^{-1} to -0.0039
19 yr^{-1} that grew towards the coastline. This result is obtained despite the buffering
20 capacity increasing in the coastal waters further inland as shown by the increase in
21 alkalinity by $1.1 \pm 0.7 \mu\text{mol kg}^{-1} \text{ yr}^{-1}$ and $2.6 \pm 1.0 \mu\text{mol kg}^{-1} \text{ yr}^{-1}$ in the inner and outer *Ría*
22 *de Vigo* respectively, driven by interannual changes in the surface salinity of
23 $0.0193 \pm 0.0056 \text{ psu yr}^{-1}$ and $0.0426 \pm 0.016 \text{ psu yr}^{-1}$ respectively. The loss of the vertical
24 salinity gradient in the long-term trend in the inner ria was consistent with other
25 significant biogeochemical changes such as a lower oxygen concentration and
26 fertilization of the surface waters. These findings seem to be related to a growing
27 footprint of sediment remineralization of organic matter in the surface layer of a more
28 homogeneous water column.

29 Data are available at: <http://dx.doi.org/10.20350/digitalCSIC/12498> (Pérez et al., 2020).

30
31 **2. Introduction**

32 Emissions of anthropogenic origin CO_2 (fossil fuels, land use and cement
33 manufacturing) into the atmosphere are the main cause behind the warming of the Earth
34 due to the greenhouse effect (IPCC, 2013). Given the constant exchange of gases
35 through the air-sea interface, the oceanic reservoir plays a key role as a sink for about

36 31% of anthropogenic CO₂ emissions (Sabine et al., 2004), controlling the partial
37 pressure of carbon dioxide in the atmosphere and regulating global temperatures.

38

39 The CO₂ uptake by the oceans produces changes in the inorganic carbon system in spite
40 of being partially dampened by the seawater buffering capacity. This ability of seawater
41 to withdraw anthropogenic CO₂ becomes more limited as more CO₂ is absorbed, which
42 will make it difficult to stabilize atmospheric CO₂ in the future (Orr et al., 2009). The
43 gradual absorption of atmospheric CO₂ by the oceans decreases seawater pH, causing
44 ocean acidification, which conditions the buffering capacity of seawater and in turn the
45 exchange of CO₂ between the ocean and the atmosphere (Caldeira and Wickett, 2003;
46 Raven et al., 2005). This effect of CO₂ absorption, which is known as ocean
47 acidification, conditions the buffering capacity of seawater and to some extent the
48 exchange of CO₂ between the ocean and the atmosphere. The Intergovernmental
49 Oceanographic Commission of the UNESCO identified the chemical change in
50 seawater brought about by ocean acidification as an indicator of a stressor on marine
51 ecosystems with a negative impact on socio-economic activities such as fishing and
52 shellfish farming. Hence, it was necessary for the oceanography community to observe
53 and gather data about pH and other parameters of the marine carbon system to conduct
54 accurate measurements of pH and ancillary parameters and provide data products to
55 help a sustainable management of the marine resources. The effect of ocean
56 acidification on marine ecosystems has stimulated impetus in the international
57 community for gathering high quality time-series measurements of the marine inorganic
58 carbon system (Hofmann et al., 2011; Andersson and MacKenzie, 2012; McElhany and
59 Busch, 2013; Takeshita et al., 2015; Wahl et al., 2016) and for predicting the future
60 evolution of the pH caused by climate change.

61

62 The threat for oceanic acidification of marine ecosystems is especially significant in
63 regions like coastal upwelling areas, which are more sensitive and appear to respond
64 faster to anthropogenic perturbations (Feely et al., 2008; Gruber et al., 2012; Lachkar,
65 2014; Hauri et al., 2013). These ecosystems are characteristic for their complex physical
66 and biogeochemical interactions and for sustaining enormous biological productivity
67 and productive fisheries (Pauly and Christensen, 1995; Hauri et al., 2009). The
68 photosynthetic activity in these regions is also an important mechanism for the seawater
69 CO₂ uptake, converting most of these areas into atmospheric CO₂ sinks (Pérez et al.,

70 1999; Cobo-Viveros et al., 2013). However, the high physical/chemical variability in
71 short temporal and spatial scales of upwelling systems and the lack of regular sampling
72 in these waters prevents a complete picture of the acidification of these ecosystems.

73

74 In the Iberian Upwelling System, the researchers of the Instituto de Investigaciones
75 Mariñas (IIM-CSIC) since 1976 commenced accurate measurements of marine
76 inorganic carbon system and associated parameters. As a result, a collection of pH
77 observations and ancillary biogeochemical information along the Galicia coast (40°N
78 and 45°N, 11°W) has been gathered under the framework of different projects over the
79 past 40 years. The current database, hereinafter called ARIOS (Acidification in the rias
80 and the Iberian continental shelf) database, holds biogeochemical information from
81 3,357 oceanographic stations, giving 17,653 discrete samples. This unique collection is
82 a starting point for evaluating the ocean acidification in the Iberian Upwelling System
83 characterized by intense biogeochemical interactions as an observation-based analysis,
84 or for use as inputs in a coupled physical-biogeochemical model to disentangle these
85 interactions at the ecosystem level.

86

87 **3. Data provenance**

88 **3.1. Data spatial coverage**

89 The main characteristic of the Galician coastline, located in the north-west of the
90 Iberian Peninsula, is the *Rías Baixas*, four long coastal estuaries or rias (>2.5 km³)
91 between 42°N and 43°N (Fig. 1). The water exchange between the *Rías Baixas* and open
92 waters is drastically affected by the coastal wind pattern as part of the Canary Current
93 Upwelling System (Wooster et al., 1976; Fraga 1981; Arístegui et al., 2004). Under the
94 predominance of northeasterly winds (Blanton et al., 1984) during spring-summer, the
95 surface offshore transport of surface waters leads to a rising cold, nutrient-rich, deep
96 water mass called the Eastern North Atlantic Central Water (ENACW) (Ríos et al.,
97 1992). Under these conditions, the *Rías Baixas* act as an extension of the continental
98 shelf (Rosón et al., 1995; Souto et al., 2003; Gilcoto et al., 2017), where upwelling
99 filaments extending westward export primary production from the coast into the ocean
100 (Álvarez-Salgado et al., 2001). In the opposite direction, the prevalence of northward
101 winds (Blanton et al., 1984) moves the surface waters towards the coast, where they
102 accumulate, sink and thus isolate the coast. This process, known as downwelling, is
103 typical during the autumn-winter along with other characteristics such as the warm,

104 salty waters from the Iberian Poleward Current (IPC) of subtropical origin (Fraga et al.,
105 1982; Alvarez-Salgado et al., 2006) that flows constrained to the Iberian shelf break
106 (Frouin et al., 1990). The run-off from local rivers also contributes to the presence of
107 river plumes over the shelf (Otero et al., 2008). These hydrodynamic conditions, the
108 meteorological forcings and the alternation of periods of upwelling and downwelling
109 (Álvarez, 1999; Gago et al., 2003c; Cobo-Viveros et al., 2013) stimulate the
110 development of intense primary production and high rates of recycling and downward
111 carbon export (Alonso-Pérez and Castro, 2014). The result of this biogeochemical
112 variability in terms of air-sea CO₂ exchange is that the surface waters act as a net CO₂
113 sink that is especially intense and variable over the shelf compared to offshore or in the
114 inner *Rías Baixas* (Padin et al., 2010).

115

116 Besides the short-term and seasonal variability, significant changes in the long-term
117 scale have been reported in this region. In addition to changes such as the weakening
118 and shortening of the upwelling events (Lemos and Sansó, 2006; Pérez et al., 2010;
119 Alvarez-Salgado et al., 2009), the warming (González-Pola et al., 2005; Pérez et al.,
120 2010) and changes in the composition of phytoplankton (Bode et al., 2009; Pérez et al.,
121 2010), the acidification in the first 700 metres for the geographical area from the Iberian
122 Peninsula to the 20° W meridian and from 36°N to 43°N has also been observed at a rate
123 of -0.0164 pH units per decade (Ríos et al., 2001; Castro et al. 2009).

124

125 **3.2. Distribution of sampling**

126 According to the type of region under study, different areas were identified in order to
127 classify the measurements gathered in the oceanographic cruises (Fig. 1). The latitude
128 of 43°N where Cape Finisterre is located was used as the dividing line between northern
129 and southern waters. Subsequently, a criterion of depth also split the waters to the north
130 of 43°N into north oceanic (below 250 m), north shelf (between 205 m and 75 m) and
131 north coast (75 m to the surface). The southern shelf waters were divided by latitude
132 42°N into Portuguese and the *Rías Baixas* (RB) shelves, whereas the shallower waters
133 were identified by the main rias, where three different zones were defined using
134 longitude boundaries (outer, middle and inner) according to Gago et al. (2003c) in the
135 *Ría de Vigo*, and just two zones in the other rias (*Ría de Pontevedra*, *Ría de Arousa*, *Ría*
136 *de Muros*). Southern waters between the isobath at 75 metres and the mouth of the
137 estuaries were identified as the Portuguese and RB coast.

138

139 The discrete measurements gathered in the ARIOS dataset were mainly found in
140 different regions' waters around 42°N latitude (Fig 1; Fig. 2a), especially in the outer
141 and middle areas of the *Ría de Vigo*, which accounted for 15% and 21% of the total
142 measurements respectively due to the proximity to the *Instituto de Investigaciones*
143 *Mariñas* (IIM-CSIC). Most of the measurements (85%) carried out by many of these
144 cruises to study the coastal ecosystems concentrated on shallow waters between the
145 seawater surface and 75 metres in depth (Fig. 2b). Although waters below 4,900 metres
146 deep were also sampled, observations below 900 metres only account for 1% of the
147 ARIOS database.

148

149 The observations made over more than 40 years in every region of the ARIOS database
150 were irregular on both an interannual and seasonal scale (Fig. 2a). The period of most
151 sampling activity was the 80s and 90s, whereas samples were especially scarce in the
152 early 2010s. On a seasonal scale, summer and autumn were the preferred seasons to
153 address the different research purposes, with 37% and 36% of the total samples
154 respectively. The observations taken during less favourable winter conditions,
155 especially aboard the coastal vessels usually available, only accounted for the 10% of
156 the ARIOS database.

157

158 **3.3. Data sources**

159 The ARIOS database is a compilation of biogeochemical properties with discrete
160 measurements of temperature, salinity, oxygen, nutrients, alkalinity, pH and chlorophyll
161 that were sampled in waters off the northwest of the Iberian Peninsula from 1976 to
162 2018 and measured by IIM-CSIC (Table 1). This data collection is part of the research
163 by 24 projects and oceanographic cruises conducted in response to different aims. The
164 different sampling strategies built up an irregular biogeochemical database whose
165 particular frequency and spatial coverage is shown in Figure 2.

166

167 The contribution to the ARIOS database from the oceanographic cruises and projects
168 over the different decades is described below.

169

170 **Cruises in the 70s and 80s:**

171 The first three cruises were carried out over three periods (1976, 1981-1983 and 1983-
172 1984), sampling the *Ría de Vigo*. These cruises were designed to provide environmental
173 information (upwelling events, estuarine circulation, continental inputs, etc.) for
174 research into the biology of some fish species. They measured identical parameters in
175 the Vigo estuary but at different stations and frequency.

176

177 In the summer of 1984, the *Galicia VIII* cruise studied the summer upwelling events
178 occurring on the contact front between the two ENACW water masses off Cape
179 Finisterre from short sections perpendicular to the Galician coast with 85 stations
180 offshore and 35 stations over the shelf. This cruise marked a milestone in the
181 oceanographic research of IIM-CSIC because it was the first time that the parameters of
182 the carbon system were measured on-board in offshore waters. Moreover,
183 measurements of a particular station on the shelf break with a bottom depth of 600
184 metres were taken every two days for a month, including two-day continuous
185 samplings.

186

187 Two years later, the *Ria de Vigo 1986* sampled along the main axis of the *Ria de Vigo*
188 in 7 monthly repetitions during the first half of the year in which the primary production
189 and the organic matter exchange between the estuary and the shelf was studied in
190 relation to the hydrographic regime. Shortly afterwards, the same topic was also
191 researched by the *Galicia IX* project in September and October 1986 from 145 stations,
192 50 of which were coastal and 80 located in ocean waters (Prego et al., 1990).

193

194 The following year, the 1987 *Provigo* project (Nogueira et al., 1997) initiated a periodic
195 study from a fixed site (42°14.5'N, 8°45.8'W) located in the main channel in the middle
196 zone of the *Ría de Vigo*. This oceanographic station was selected as suitable for
197 evaluating the main processes that occur in the inner ria associated with external forcing
198 changes (Rios, 1992; Figueiras et al., 1994). Although the *Provigo* project finished in
199 1996, the fixed station was repeatedly included in subsequent cruises, extending the
200 time series at this location until today, when it is currently sampled every week by
201 INTECMAR (www.intecmar.gal). An example of the subsequent sampling repetition of
202 this station occurred the following year when one of the three stations in the Vigo
203 estuary in the *Luna 1988* project (Fraga et al., 1992) took a sample every two weeks to

204 study the environmental control over the phytoplankton populations throughout an
205 annual cycle (February 1988 - February 1989).

206

207 At the end of 80s, the carbon system monitoring by the IIM-CSIC was extended to the
208 *Ría de Arousa* throughout 1989 (Álvarez-Salgado et al., 1993; Perez et al., 2000) in
209 order to learn the effect of upwelling on the water circulation pattern, community
210 production and the fluxes and net budgets of biogenic constituents in this ria with the
211 highest mussel production in Europe. For 5 months, 11 stations' samples were repeated
212 twice a week in the ria that is the most productive, housing intense cultivation of
213 mussels on rafts (Blanton et al., 1984).

214

215 **Cruises of the 90s:**

216 In the first half of this decade, studying the phytoplankton communities was the
217 oceanographic cruises' most relevant aim, concentrating particularly on harmful algae
218 blooms. The hydrodynamic and biogeochemical conditions controlling the growth,
219 development and migration of the phytoplankton were analysed both in the interior of
220 the estuary and on the continental shelf.

221

222 For five days in September, the 1990 *Ría de Vigo* cruise (Figueiras et al., 1994) sampled
223 five stations distributed along the longitudinal axis of the ria and one at the northern
224 mouth. The next year, the cruise Galicia XI was carried out in May, sampling at 39
225 stations along eight transects perpendicular to the coastline; and Galicia XII (Alvarez-
226 Salgado et al., 1998, 2002, 2003; Castro et al., 1994) in September, sampling at 37
227 oceanic stations and 7 coastal stations.

228

229 The *Ría de Vigo* cruise in 1993-4 (Miguez et al., 2001), with four stations using 24
230 repetitions with a CTD-SBE25, investigated the hydrodynamic and biogeochemical
231 effect on the evolution of phytoplankton communities in the *Ría de Vigo*. Six samples
232 were taken in approximately two weeks corresponding to two different periods
233 (27 September to 8 October 1993, and 6 March to 24 March 1994).

234

235 *Ría de Vigo* 1994-95 (Alvarez et al., 1999; Doval et al., 1998, 1997a, 1997b) and *Ría de*
236 *Vigo* 1997 (Gago et al., 2003a, b, c) were two cruises that took place in the second half
237 of the decade. These campaigns' objective was no longer the ecology of the plankton,

238 but the factors behind the variation of the carbon pools during the upwelling and
239 downwelling events along the central axis of the *Ría of Vigo*. During the 1997 cruises
240 on board the *B/O Mytilus*, a systematic observation of the pCO₂ was carried out for the
241 first time in Spanish coastal waters, using an autonomous continuous system with
242 additional measurements of temperature, salinity and chlorophyll.

243

244 **Cruises in the 2000s and recent years:**

245 After a period of poor sampling at the end of 90s, the first decade of the 21st century
246 gave new impetus to biogeochemical monitoring of Galician waters. As shown below,
247 several projects dealt with various objectives, focussing on particular issues in the
248 dynamics of these waters:

249

250 The DYBAGA project (Galician Platform's Annual Dynamics and Biochemistry: short-
251 scale variation) (Álvarez-Salgado et al., 2006; Castro et al., 2006; Nieto-Cid et al.,
252 2004) analysed the phenomena of upwelling and downwelling in the Galician shelf
253 opposite the *Ría de Vigo* weekly and their impact on the different biogeochemical and
254 carbon system variables including organic dissolved matter. Three stations were
255 sampled weekly from May 2001 to April 2002 between the shelf break (1,200 m deep)
256 to the middle of the *Ría de Vigo* (45 m deep).

257

258 The REMODA (Reactivity of dissolved organic matter in a coastal upwelling system)
259 (Álvarez-Salgado et al., 2005; Piedracoba et al., 2005; Nieto-Cid et al., 2006) project
260 concentrated on learning the origin and destination of dissolved organic matter in the
261 *Ría de Vigo* as well. Three stations along the main axis of the *Ría de Vigo*, including the
262 fixed station as the central one, took samples with short (3-4 days) and seasonal time
263 scales.

264

265 The FLUVBE project (Coupling of benthic and pelagic fluxes in the *Ría de Vigo*) added
266 to knowledge about the productivity and the benthic fluxes of oxygen and inorganic
267 nutrients in the *Ría de Vigo* from 16 oceanographic surveys with four stations between
268 April 2004 and January 2005.

269

270 The ZOTRACOS project studied the biogeochemical and hydrodynamic
271 characterization of the coastal transition zone in NW Spain during the downwelling
272 period (Teira et al., 2009).

273

274 The CRIA (Circulation in a RIA) (Barton et al., 2019) project examined the layout of
275 the two-layer circulation and propagation of upwelled and downwelled waters in order
276 to estimate the flushing and vertical velocities in the *Ría de Vigo* in repeated
277 hydrographic surveys between September 2006 and June 2007 (Barton et al., 2015,
278 2016; Alonso-Perez and Castro, 2014; Alonso-Perez et al., 2010; Alonso-Perez et al.,
279 2015).

280

281 The RAFTING project (Impact of mussel raft cultivation on the benthic-pelagic
282 coupling in a Galician ria) (Frojan et al., 2018; Frojan et al., 2016; Froján et al., 2014)
283 assessed for the first time how mussel cultivation influences the quality of particular
284 organic carbon fluxes in the *Ría de Vigo*. Over the four seasons, two stations were
285 visited every two to three days during each period, meaning 24 oceanographic cruises in
286 2007 and 2008.

287

288 The CAIBEX (Continental shelf-ocean exchanges in the marine ecosystem of the
289 Canary Islands-Iberian Peninsula) (Villacieros-Robineau et al., 2019) project compared
290 the dynamics and biogeochemical activity between the coastal zone and the adjacent
291 ocean in the study zone during the summer upwelling events. As part of the CAIBEX
292 project, a mooring at the LOCO (Laboratory of Ocean and Coastal Observation)
293 (Zuñiga et al., 2016, 2017) site located on the continental shelf was deployed and visited
294 monthly for one year to monitor the vertical profiles of biogeochemical variables.

295

296 After these projects were completed in 2009, new measurements were not provided
297 until 2018. The aim of the ARIOS project (Acidification in the rias and on the Iberian
298 continental shelf) was to evaluate the impact of ocean acidification and learn about
299 potential impacts on the mussels and their adaptation (Lassoued et al., 2019) to the new
300 climate change.

301

302 **3.4. Methods**

303 To assess of the level of acidification in the ocean adjacent to the Galician coast,
304 variables of the carbon system (pH and alkalinity), nutrient concentration, dissolved
305 oxygen, chlorophyll-a, salinity and temperature were measured in each cruise. The
306 variables measured in each oceanographic cruise gathered in the ARIOS dataset are
307 shown in Table 1. The main changes in the material and methods throughout these years
308 are detailed below.

309

310 **T-S measurements**

311 Temperatures from 1976 to 1984 were measured using a Wallace and Tiernan
312 bathythermograph. Reversing thermometers that had a precision of 0.02°C were used,
313 attached to the water samplers between 1984 and 1990, correcting the temperature
314 between the protected and unprotected thermometers according to Anderson (1974).
315 During those years, the depth was calculated from the thermometric readings, rounding
316 the result off to the nearest ten. After 1990, different models of CTD instruments that
317 measured the seawater temperature with a precision of 0.002°C were used to obtain the
318 thermohaline profile.

319

320 The first measurements of salinity were determined with a Plessey Environmental
321 Systems 6230N inductive salinometer calibrated with normal IAPSO water and
322 calculated from the equations given in the NIO and UNESCO International
323 Oceanographic Tables (1981). The precision of these salinity measurements was 0.005
324 psu. After using this equipment, the salinity was determined with an AUTOSAL 8400A
325 inductive salinometer calibrated with normal IAPSO water whose estimated analytical
326 error was 0.003, using the equation of practical salinity given by UNESCO (1981).
327 CTDs began to be used in 1990 to record the vertical salinity profiles, calibrated using
328 the salinity samples, whose possible deviations in the measurements were estimated
329 from the discrete measurements from the AUTOSAL salinometer.

330

331 **pH measurements**

332 The pH measurements were originally taken with a Metrohm E-510 pH meter with a
333 glass electrode and a Ag/ClAg reference one calibrated with 7.413 NBS buffer. All pH
334 values were converted to values at 15 °C using the temperature correction from the
335 Buch and Nynas tables published by Barnes (1959). In 1984, the method was modified
336 and the temperature normalization was carried out following Pérez and Fraga (1987b).

337 Two years later, the measurement equipment was the Metrohm E-654 pH meter with an
338 Orion 81-04 Ross combined glass electrode, with the pH converted to the SWS scale
339 using the hydrogen activity coefficient given by Mehrbach et al. (1973) at 25°C with the
340 parameterization given by Pérez and Fraga (1987b). The error in this potentiometric
341 method was 0.010. In 2001, the seawater pH measurements were determined with a
342 spectrophotometric method following Clayton and Byrne (1993), subsequently adding
343 0.0047 to the pH value according to DelValls and Dickson (1998). The precision of the
344 spectrophotometric measurements was 0.003 pH units.

345

346 The pH values were reported on total pH scale at 0 dbar of pressure and both at 25°C
347 and in situ temperature (pH_T) following the same procedure of GLODAP v2 (Olsen et
348 al., 2019). A total of 12,220 measurements of pH on NBS scale were converted to the
349 total scale using CO2SYS (Lewis and Wallace, 1998) for MATLAB (van Heuven et al.,
350 2011) with pH and total alkalinity as inputs. The conversion was conducted with the
351 carbonate dissociation constants of Lueker et al. (2000) and the borate-to-salinity ratio
352 of Uppström (1974). Whenever total alkalinity data were missing, these values were
353 approximated as 66 times salinity that is the mean ratio between the total alkalinity and
354 the salinity of every in situ measurements compiled in the ARIOS database. Data for
355 phosphate and silicate are also needed and were, whenever missing, a constant values of
356 $10 \mu\text{mol kg}^{-1}$ for silicate and $1 \mu\text{mol kg}^{-1}$ for phosphate were used. These
357 approximations were tested on 8,296 samples with complete biogeochemical
358 information showing a bias of less than 0.0004 pH units for 99.95% of the samples.

359

360 **Alkalinity measurements**

361 The seawater alkalinity was measured for the first time in 1981 by potentiometric
362 titration with HCl 0.1M at final pH 4.44 following Pérez and Fraga (1987a) with an
363 analytical error of $2 \mu\text{mol kg}^{-1}$ and a precision of 0.1%. Sodium tetraborate decahydrate
364 (Borax, $\text{Na}_2\text{B}_4\text{O}_7 \cdot 10\text{H}_2\text{O}$, Merck p.a.) was used for standardizing the HCl (0.13 M). The
365 pH measurements were carried out with a combined glass electrode (Metrohm E-121)
366 with Ag/AgCl (KC1 3M) as the reference. The pH was calibrated using the NBS buffers
367 assuming the theoretical slope. As of 2001, the accuracy of alkalinity measurements
368 was determined using samples of certified reference material (CRM) provided by Dr. A.
369 Dickson, University of California, improving the precision to $\pm 1.4 \text{ mol kg}^{-1}$ and an

370 accuracy of <0.1% recently established by (Ríos and Pérez, 1999) from cross-
371 calculation with measured Certified Reference Materials (Dickson et al., 2007).

372

373 **Nutrient measurements**

374 Except for the Galicia cruises (Table 1), in which nutrient samples were analysed on
375 board, samples were kept in the dark and cold (4°C) after collection for further analyses
376 in the shore based laboratory. Nutrient concentration was determined by a flow-
377 segmented autoanalyzer (Technicon AAI and Alpkem after 1995) as described in
378 Strickland and Parsons (1968) with the particularity that the reduction of nitrate to
379 nitrite with Cd column was done using a citrate buffer according to Mouriño and
380 Fraga's modification (1985). Phosphates and silicates were measured following
381 Grasshoff (1983), and ammonium as described by Grasshoff and Johannsen (1972).
382 This method was maintained in the subsequent cruises, achieving a precision of 0.02
383 $\mu\text{mol/kg}$ for nitrite, 0.1 $\mu\text{mol/kg}$ for nitrate, 0.05 $\mu\text{mol kg}^{-1}$ for ammonium and silicate,
384 and 0.01 $\mu\text{mol/kg}$ for phosphate.

385

386 **Oxygen measurements**

387 The dissolved oxygen was determined via the Winkler titration method for the first time
388 in 1981 following the procedure published later by Culberson et al. (1991). The oxygen
389 concentration in the samples in this method was fixed with MnCl_2 and NaOH/NaI ,
390 which were kept in the dark until analysis in the laboratory 12-24 hours later. The
391 measurements were made by titration of iodine with thiosulfate using an automatic
392 titrator. During the 80s and early 90s, the titration was carried out with Metrohm
393 instruments (E-425 or E-473), which had an analytical error of 1 $\mu\text{mol kg}^{-1}$. The oxygen
394 concentration after 1997 was estimated using a Titrino 720 (Metrohm) analyser with an
395 accuracy of 0.5 $\mu\text{mol kg}^{-1}$.

396

397 **Chlorophyll measurements**

398 The chlorophyll-a values were measured following SCOR-UNESCO (1966) using a
399 6 cm diameter Schleicher and Scholl 602eh filter covered with magnesium carbonate.
400 The absorption was measured in 1 cm optical path cuvettes using a Beckman DU
401 spectrophotometer. In 1984, discrete water samples of the chlorophyll-a samples were
402 filtered through Whatman GF/F filters of 2.5 μm , which were preferred from then on,
403 and measured fluorometrically following Strickland and Parsons (1972) without

404 correction for concentration by pheophytes. The fluorescence readings were carried out
405 with a Turner Designs 10,000 R fluorometer (Yentsh and Menzel, 1963) obtaining a
406 precision of 0.05 g L⁻¹.

407

408 **Quality control**

409 Every cruise gathered in Table 1 passed 1st quality control (QC1) to ensure truly
410 confident results. The GO-SHIP software for quality control of hydrographic data (Velo
411 et al., 2019) that compile several QC1 procedures was applied to ARIOS dataset. That
412 procedures consist on reviewing the property profiles and property-property plots
413 generated by that application, adequate for each variable. A quality control flag value
414 following the recommendations from WOCE bottle data flagging quality codes was
415 assigned to each measurement available from the repository sites (Table 1). This
416 method was preferred over applying a very stringent flagging process because it is
417 difficult to rule out some extreme values associated with low salinities or that could be
418 supported by the high variability of an ecosystem characterized by an intense biological
419 activity. Nutrients and chlorophyll with values inferior to the precision were flag=2.
420 Some very low pH associated to very low salinity waters were flagged as doubtful.

421

422 The ARIOS database includes the cruise corrections for pH data of the -0.017 for the
423 Galicia VIII cruise (29GD19840711) and +0.032 for Galicia IX cruise
424 (29GD19860904) detected during the second level quality control of CARINA project
425 (Velo et al., 2010).

426 **4. Results**

427 Some of the most obvious results provided by the ARIOS database are shown below.
428 The purpose is to describe the environmental context and the main oceanographic
429 processes that affect the variability of these discrete measurements and offer
430 preliminary information for future detailed biogeochemical research.

431

432 **4.1. Vertical distribution**

433 The vertical profile of the temperature, salinity, pH on total scale at in situ temperature
434 (pH_T), NO₃⁻ and oxygen concentration in the ocean region between 41°N and 43°N was
435 estimated for each oceanographic station as the mean value of the depth ranges
436 described in Figure 2b. These measurements were gathered attending to the collection
437 periods (December-February, March-May, June-August and September-November) and

438 averaged to describe winter, spring, summer and autumn respectively (Fig. 3, Table A1
439 in the Appendix).

440

441 The vertical distribution of the temperature (Fig. 3a) showed the presence of warmer
442 saline waters throughout the water column in winter with the exception of the surface
443 waters during summer, which showed intense heating due to the radiant solar energy.
444 Below the maximum temperature observed during the summer, cold central waters of
445 subpolar origin occupied the water columns with lower salinity (Fig. 3b). The vertical
446 variation of temperature is typical for a temperate region with relatively homogenous
447 deep water below the seasonal thermocline, reaching maximum SST values in summer
448 and autumn, and minimums in spring and winter. The winter temperature profile is
449 relatively warmer than in spring because of the presence of the IPC (Alvarez-Salgado et
450 al., 2006), which reaches a depth of 300 metres. The maximum salinity is also found in
451 winter due to the presence of the IPC, whereas the minimum values are found in autumn
452 (Fig. 3b). Below 500 metres in depth, the increase in salinity points to the presence of
453 Mediterranean Water. These differences reach a minimum at 500 metres deep, where
454 the salinity values coincided. From this depth down to 1,100 metres, the differences in
455 temperature and salinity throughout the four seasons were minimal, with the mean
456 values converging to $11.03 \pm 0.07^\circ\text{C}$ and 36.117 ± 0.009 psu, respectively (Fig. 3ab).

457

458 The vertical profiles of pH_T , NO_3^- and oxygen concentration (Fig. 3cde) also showed a
459 variation lower than 1% within this depth range with annual means of $15.2 \pm 0.1 \mu\text{mol}$
460 kg^{-1} , 8.025 ± 0.005 and $188 \pm 1 \mu\text{mol kg}^{-1}$ respectively. The pH values from a maximum
461 subsurface located at around 40 metres deep showed a clear inverse correlation with the
462 depth down to a depth of 500 metres throughout the seasonal cycle, where the annual
463 minimum value of 8.018 ± 0.005 was reached. The higher pH values could be attributed
464 to the biological reduction of CO_2 by phytoplankton activity, which brought the pH to a
465 maximum value of 8.13 to 40 meters during the spring bloom. After the intense
466 photosynthetic activity observed in surface waters during spring and summer, pH values
467 reached minimum values in the first 200 metres of depth during autumn due to
468 respiration of organic matter. However, it was at a depth of 500 metres that the
469 minimum pH values were measured in all seasons where is found the subpolar Eastern
470 North Atlantic Central Water proceeding from the northeastern cyclonic gyre (Harvey,
471 1982; Ríos et al., 1992). The influence of phytoplankton growth on biogeochemistry

472 during spring can be also evidenced by the oxygen concentration pattern (Fig. 3e). In
473 the upper layer above 250 metres depth, spring oxygen levels exceeded those in winter,
474 whereas a decrease in oxygen concentration was found from this depth down to 1000
475 metres, possible due to enhanced respiration from cascading organic matter. The impact
476 on the growth of the phytoplankton community during the spring was also evident,
477 judging by the oxygen concentration. So, in the upper waters the spring oxygen
478 concentration values exceeded those of the winter values, while oxygen consumption
479 was found from a depth of 300 metres to 1,000 metres due to respiration from organic
480 matter arriving from above. The minimum values for oxygen concentration throughout
481 the water column were found during summer and autumn. The nitrate concentration
482 displayed a particularly vertical distribution, growing with depth from minimum values
483 in the upper layer of the ocean region, which was practically zero during the first 50
484 metres. Below 100 metres, the nitrate concentration showed the maximum values in the
485 vertical distribution during summer and autumn coinciding with the presence of waters
486 of subpolar and subtropical origin respectively, whereas the minimum values appeared
487 in winter. Towards the bottom, the seasonal values of NO_3^- concentration were almost
488 coincident at a mean value of $15.2 \pm 0.1 \mu\text{mol kg}^{-1}$.

489

490 **4.2. Seasonal cycle**

491 The seasonal cycle of the biogeochemical properties (temperature, salinity, pH_T , oxygen
492 concentration, nitrate concentration and chlorophyll) in the surface waters (0 to 5
493 metres) of five geographical boxes was estimated as a monthly average previously
494 filtering values outside of two standard deviations of the mean (Table A2 in the
495 Appendix). Five regions that were located as a longitudinal transect between the inner
496 Ría de Vigo and the ocean zone are shown in Fig. 4.

497

498 In general terms, the seasonal variability of the temperature was very similar in every
499 area, ranging between 12 and 19°C (Fig. 4a). Only particular features observed on a
500 short-term scale as in the examples below differ between each region. The warmer
501 waters were usually found in the oceanic zone, reaching a maximum monthly averaged
502 temperature of 18.6°C in September, while the coldest surface waters of 12.6°C were
503 located in the inner stations closer to the mouth of the *Ría de Vigo* in January. Another
504 secondary minimum averaged temperature was also found in the shelf and the outer area
505 of the *Ría de Vigo*, which was remarkably low in August due to the entry of cold

506 upwelled waters in the surface layer (Alvarez-Salgado 1993).

507

508 The monthly salinity averages (Fig. 4b) clearly showed significant differences between
509 the offshore and coastal waters. Sharp salinity changes were seen in the estuary during
510 winter, especially in the inner area where values lower than 28 psu were reached with
511 the arrival of continental inputs in December. The weak seasonal cycle of salinity in the
512 shelf and ocean waters showed high values in December due to the influence of warm
513 saline water from the IPC, usually located on the shelf slope even though it may even
514 enter the rias depending on the relative intensity of shelf winds and the intensity of the
515 continental runoff (Alvarez-Salgado et al., 2003). In this sense, the slight salinity
516 minimum observed in the shelf waters in March could be consequence of the offshore
517 spreading of the maximum discharges from the River Miño and Douro (Otero et al.,
518 2010) at the end of downwelling season. After this, the shelf and ocean waters showed
519 minimum values in summer due to the arrival of cooler and fresher subpolar waters
520 (Rios et al., 1992; Alvarez-Salgado et al., 2003, 2006). In August, coinciding with the
521 maximum salinity of the surface waters in the interior of the *Ría de Vigo* due to the
522 minimum river runoff, the surface waters between the inner *Ría de Vigo* and the ocean
523 region were almost homogeneous, with minimum differences in salinity of 0.2 psu.

524

525 Like salinity, there was little seasonal variability in pH in the offshore waters, but large
526 seasonal variability in coastal waters, with maximum and minimum pH values in spring
527 and autumn, respectively, and in all regions (Fig. 4c). The net balance between
528 production and respiration of organic matter and the estuarine circulation caused a
529 maximum pH of 8.19 in the outer region of the *Ría de Vigo* in May and a minimum of
530 7.96 in the inner waters in November.

531

532 The oxygen concentration (Fig. 4d) in the coastal ecosystems is also controlled by the
533 remineralization of the organic matter and photosynthetic activity of the phytoplankton
534 community, with the effect of salinity and temperature on the oxygen saturation level.
535 The variability in the oxygen concentration, like the pH distribution, showed a growing
536 seasonal amplitude towards the coastline, with maximum values in the outer and middle
537 *Ría de Vigo* and lower values in the inner waters, especially during the second half of
538 the seasonal cycle. Hence, the dissolved oxygen concentration mirrored the seasonal
539 cycle of pH, showing growing seasonal amplitude towards the coastline with a range

540 between 284 $\mu\text{mol kg}^{-1}$ found in the outer region of the *Ría de Vigo* in May and 205
541 $\mu\text{mol kg}^{-1}$ in the inner waters in November. These results seem to reinforce the
542 importance of the oxygen consumption in this shallow area, where the water column is
543 less than 10 metres deep and therefore it would also be influenced by benthic respiration
544 (Alonso-Pérez and Castro, 2014).

545

546 The monthly means of nitrate concentration (Fig. 4e) could be summarized as high
547 values during autumn and winter due to the nutrients delivered from the continent and
548 the vertical mixing, and as minimum nitrate values from March to September because of
549 phytoplankton consumption. The nitrate concentration was markedly higher in the inner
550 *Ría de Vigo*, where it exceeded 9 $\mu\text{mol kg}^{-1}$ in February and decreased towards the open
551 ocean, where the highest monthly value was seen to be 2.5 $\mu\text{mol kg}^{-1}$. Some notable
552 aspects can be seen in Fig. 5d, such as water poor in nitrate in the ocean region between
553 the two peaks of 3.5 $\mu\text{mol kg}^{-1}$ in March and 1.3 $\mu\text{mol kg}^{-1}$ in October. This shows the
554 presence of the IPC waters, which are warmer and saltier than the shelf waters. Also
555 noteworthy was the particular fact that while the nitrate concentration in other areas was
556 practically zero in summer, the nitrate amount in the surface waters within the *Ría de*
557 *Vigo*, and especially in the inner *Ría de Vigo*, was not completely consumed. This
558 indicates a constant supply throughout the year, either through upwelling events or the
559 continental inputs. This in turn means that while the chlorophyll values were at a
560 minimum in the offshore waters in summer, the phytoplankton community in the
561 estuary grew in summer during the upwelling relaxation periods (Pérez et al., 2000).
562 The nutrient concentration during spring and summer was only detectable in the newly
563 upwelled waters that can show values up to 6 $\mu\text{mol L}^{-1}$ (Fraga, 1981; Castro et al.,
564 1994). During the cessation of the upwelling season in September and October, the
565 chlorophyll concentration (Fig. 5f) increased again, sustained by nutrients that entered
566 from deeper waters through vertical mixing. It should be noted that there was a
567 coincidence of high chlorophyll in the water column and low oxygen concentration in
568 the inner *Ría de Vigo* from May to November, indicating the potential importance of
569 benthic fluxes and vertical fluxes (reference).

570

571 **4.3. Long-term trends**

572 The long-term trends of the biogeochemical properties in the surface waters along the
573 described longitudinal transect between the inner *Ría de Vigo* and the ocean zone were

574 estimated to be the interannual linear rate of the deseasonalized time series, previously
575 removing the monthly means in these regions and assuming a null spatial variability.
576 The significant trends in the ARIOS database, meaning long-term variability, should be
577 interpreted as a combination of the natural variability on a decadal scale (Pérez et al.,
578 2010; Padin et al., 2010) and anthropogenic forcings (Wolf-Gladrow et al., 1999;
579 Anderson and Mackenzie 2004; Bakun et al., 2010).

580

581 No long-term temperature variability was found in the surface waters of any region
582 despite the known warming previously reported on the Northern Iberian coast (Pérez et al.,
583 2010; Gesteira et al., 2011; González-Pola et al., 2005). Unlike the temperature, the
584 other expected consequence of climate change in marine ecosystems, namely ocean
585 acidification (Caldeira and Wickett, 2003) was observed along the longitudinal transect,
586 with a greater decrease in the long-term trend of pH towards the coast (Table 2). The
587 long-term pH variation of $-0.0039 \pm 0.0005 \text{ yr}^{-1}$ in the inner waters was about three fold
588 higher than the change observed in the ocean zone, equivalent to $-0.0012 \pm 0.0002 \text{ yr}^{-1}$ in
589 the ocean zone, explaining the 34% and 22% variation in pH in situ respectively, and
590 representing 1-3% of the seasonal pH variation in all zones. These pH decrease rates
591 found in both coastal and open ocean regions of the Iberian Upwelling System lie
592 within the range of other acidification rates estimated in different sites of the North
593 Atlantic Ocean (Lauvset and Gruber, 2014; Bates et al., 2014), being also coherent with
594 the mean rates calculated for the global ocean and for the Eastern North Atlantic and
595 equal to -0.018 and $-0.0164 \text{ decade}^{-1}$, respectively (Lauvset et al., 2015; Rios et al
596 2001).

597

598 The long-term trend in salinity was also seen to be evidently dependent on the distance
599 to the mouth of the *Ría de Vigo*. The interannual rate of sea surface salinity in the outer
600 and inner ria previously reported by Rosón et al. (2009) was $0.0426 \pm 0.016 \text{ psu yr}^{-1}$ and
601 $0.0193 \pm 0.0056 \text{ psu yr}^{-1}$ respectively. These changes were observed in parallel to an
602 interannual alkalinity increase that is cancelled out in the normalized alkalinity,
603 estimated as the difference between the alkalinity measured and the alkalinity calculated
604 using the linear regression with salinity in each region. Therefore, the interannual
605 salinity increase was the forcing that explains the increase in the buffer capacity of the
606 surface waters (Sarmiento and Gruber, 2006).

607

608 Other significant long-term variations were found in other biogeochemical parameters
609 in the ARIOS database. The long-term trend of the concentrations of nutrients in the
610 inner Ría de Vigo that had been previously reported for the period 2001-2011 by Doval
611 et al. (2016) showed a significant increase in nitrate, phosphate and ammonium
612 concentrations of $0.0559 \pm 0.0158 \mu\text{mol kg}^{-1} \text{ yr}^{-1}$, $0.0076 \pm 0.0016 \mu\text{mol kg}^{-1} \text{ yr}^{-1}$ and
613 $0.0560 \pm 0.0011 \mu\text{mol kg}^{-1} \text{ yr}^{-1}$ respectively. This fertilization on a long-term scale in the
614 surface waters of the inner ria estimated from ARIOS database was observed in parallel
615 to the deoxygenation of $-0.7 \pm 0.2 \mu\text{mol kg}^{-1} \text{ yr}^{-1}$. The apparent oxygen utilisation
616 (AOU), calculated using the concentration of O_2 at saturation calculated according to
617 Benson and Krause (1984), underwent an equivalent significant long-term change of
618 $0.7 \pm 0.2 \mu\text{mol kg}^{-1} \text{ yr}^{-1}$, indicating that either the biological consumption rates, or a
619 change in the amount of time that the waters are ventilated, or even its interaction or
620 exchange with the sediment, cause the the long-term reduction of oxygen.

621

622 This fertilization on a long-term scale estimated from ARIOS database in the surface
623 waters of the inner ria was observed in parallel to the deoxygenation of $-0.7 \pm 0.2 \mu\text{mol}$
624 $\text{kg}^{-1} \text{ yr}^{-1}$. The apparent oxygen utilisation (AOU), calculated using the concentration of
625 oxygen at saturation calculated according to Benson and Krause (1984), underwent a
626 long-term change of $0.7 \pm 0.2 \mu\text{mol kg}^{-1} \text{ yr}^{-1}$ equal to the observed in the measurements
627 of oxygen concentration. This coincidence may indicates that the long-term reduction of
628 oxygen is due to the changes in the biological consumption rates, in the rates of the
629 waters ventilation or even in sediment-water interactions rather than due to the effect of
630 temperature. and salinity on oxygen saturation.

631

632 These findings found in the shallower waters of the *Ría de Vigo* allow us to hypothesize
633 that the long-term increase in salinity would produce an increasingly weak vertical
634 salinity gradient in the water column that would favour the vertical fluxes between the
635 bottom and surface waters. Therefore the observed changes of oxygen and
636 remineralized nutrient inputs in the surface waters could be due to an increasing
637 footprint of benthic respiration, that has a major importance in the net ecosystem
638 metabolism of this coastal region (Alonso-Pérez et al., 2015). This hypothesis would
639 also explain the intense acidification in the inner waters in spite of growing alkalinity
640 buffering.

641

642 The mean values at each station of the ARIOS database estimated for each depth range
643 described in Figure 2, resulting in 8,384 values, were used to estimate a general value of
644 the long-term trend in pH. The historical pH values in situ from the ARIOS database
645 showed a general decrease in seawater pH in the Iberian Upwelling between 1976 and
646 2018, with an acidification rate of $-0.012 \pm 0.002 \text{ yr}^{-1}$ that significantly explains 2% of
647 the total pH variation (Fig. 5a). The apparent oxygen utilisation was also shown as
648 function of pH over time, revealing the association of higher AOU values with lower
649 pH. The relationship between pH and AOU (Fig. 5b) showed an inverse linear
650 correlation of $-399 \pm 5 \text{ } \mu\text{mol kg}^{-1}$ and a coefficient of determination (r-squared) of 0.52.
651 The strong biological activity of the upwelling systems is the main driver of pH
652 changes, explaining 52% of the observed variation in the discrete measurements. The
653 distribution of nitrate seen in relation to the distribution of pH and AOU (Fig. 5b)
654 showed the association of higher pH values with negative AOU values and a nitrate
655 decrease, reinforcing the importance of biological processes in these marine carbonate
656 system. Although the different processes controlling the AOU values were not separated
657 in this analysis, the oxygen concentration in addition to the remineralization of the
658 organic matter and the photosynthesis is conditioned by changes in temperature and
659 salinity, ventilation events, water masses mixing and other processes (Sarmiento and
660 Gruber, 2006). Therefore, the long-term drop in seawater pH measurements estimated
661 from the ARIOS database presented here confirms that the future evolution of ocean
662 acidification in this productive region is likely to depend on both the CO₂ increase in
663 the atmosphere and other long-term changes (of natural and/or anthropogenic origin)
664 affecting the seawater's carbonate system.

665

666 **5. Data availability**

667 The ARIOS dataset (Pérez et al., 2020) is archived at DIGICAL CSIC under the Digital
668 Object Identifier (DOI): <http://dx.doi.org/10.20350/digitalCSIC/12498>.

669

670 The data are available as WHP-Exchange bottle format (arios_database_hy1.csv). A
671 documentation file (readme_ARIOSDATABASE.txt) provides an description of the
672 material and methods of the measurements and the parameters of the dataset. In both
673 files, a table similar to the Table 1 of this manuscript include the DOI and the
674 EXPOCODE of the original cruise files gathered in the ARIOS dataset.

675

676 These data are available to the public and the scientific community with the aim of that
677 their wide dissemination will lead to new scientific knowledge about the ocean
678 acidification and the biogeochemistry of the Galicia Upwelling System. The dataset is
679 subject to a Creative Commons License Attribution-ShareAlike 4.0 International
680 (<http://creativecommons.org/licenses/by-sa/4.0/>) and users of the ARIOS dataset should
681 reference this work.

682

683 **6. Conclusions**

684 The ARIOS database is a unique compilation of biogeochemical discrete measurements
685 in the Iberian Upwelling Ecosystem from 1976 to 2018. This data set comprises more
686 than 17,653 discrete samples from 3,357 oceanographic stations (but not always for all
687 parameters) of pH, alkalinity and associated physical and biogeochemical parameters
688 (e.g., temperature, salinity, and chlorophyll and oxygen concentrations). The material
689 and methods varied throughout the sampling period due to logistical and analytical
690 issues such as those described in Table 1, where different sites are mentioned to
691 download these measurements and detailed information.

692

693 Among the results described as preliminary and relevant information to learn the
694 environmental and oceanographic context of the ARIOS database, we can mention the
695 following main points concerning the pH characteristics of the Iberian Upwelling
696 System:

- 697 • A decrease in seawater pH in the Iberian Upwelling between 1976 and 2018,
698 with an acidification rate of $-0.012 \pm 0.002 \text{ yr}^{-1}$ that significantly explains 2% of
699 the total pH variation
- 700 • An interannual pH variation of $-0.0039 \pm 0.0005 \text{ yr}^{-1}$ in the inner waters and -
701 $0.0012 \pm 0.0002 \text{ yr}^{-1}$ in the ocean zone.
- 702 • An inverse linear correlation between pH and AOU of $-399 \pm 5 \text{ } \mu\text{mol kg}^{-1}$ that
703 explained 52% of the observed variation in the discrete measurements.

704

705 This published ARIOS database is a useful and necessary tool to confirm and study
706 biogeochemical changes in the seawater at long term trend. Likewise, we understand
707 that it is a starting point to which to add future observation projects to continue
708 increasing the knowledge about the impact of climate change in the Iberian Upwelling
709 Ecosystem.

710

711 **Acknowledgements.**

712 The compilation of this data set was funded by the ARIOS project (CTM2016-76146-
713 C3-1-R) funded by the Spanish government through the Ministerio de Economía y
714 Competitividad that included European FEDER funds. Part of the processing work was
715 supported by the MarRISK project (European Union FEDER 0262_MarRISK_1_E)
716 funded by the Galicia-Northern Portugal Cross-Border Cooperation Program
717 (POCTEP). This project has also received funding from the European Union's Horizon
718 2020 research and innovation programme under grant agreement No 820989 (project
719 COMFORT, Our common future ocean in the Earth system – quantifying coupled
720 cycles of carbon, oxygen, and nutrients for determining and achieving safe operating
721 spaces with respect to tipping points). This data set encompasses decades of work
722 conducted by an overwhelming number of people. We thank all of the scientists,
723 technicians, personnel, and crew who were responsible for the collection and analysis of
724 the over 22 000 samples included in the final data set. In addition to the PI cited in
725 Table 1 we also thank to Trinidad Rellán, Antón Velo, Miguel Gil Coto, Marta Alvarez,
726 Marylo Doval, Jesus Gago, Daniel Broullón and Marcos Fontela. We also thank Monica
727 Castaño for starting this data compilation more than 10 years ago.

728

729 **References**

730 Alonso-Perez F., Ysebaert, T., and Castro, C. G.: Effects of suspended mussel culture
731 on benthic-pelagic coupling in a coastal upwelling system (Ría de Vigo, NW Iberian
732 Peninsula), *Journal of Experimental Marine Biology and Ecology*, 382–391,
733 <https://doi.org/10.1016/j.jembe.2009.11.008>, 2010.

734

735 Alonso-Perez, F., and Castro, C. G.: Benthic oxygen and nutrient fluxes in a coastal
736 upwelling system (Ria de Vigo, NW Iberian Peninsula): seasonal trends and regulating
737 factors. *Mar Ecol Prog Ser* 511:17-32. <https://doi.org/10.3354/meps10915>. 2014.

738

739 Alonso-Perez, F., Zúñiga, D., Arbones, B., Figueiras, F. G., and Castro, C. G.: Benthic
740 fluxes, net ecosystem metabolism and seafood harvest: Completing the organic carbon
741 balance in the Ría de Vigo (NW Spain), *Estuarine Coastal Shelf Science*, 163,
742 <https://doi.org/10.1016/j.ecss.2015.05.038>. 2015.

743

744 Alvarez-Salgado, X. A., Rosón, G., Pérez, F. F. and Pazos, Y.: Hydrographic variability
745 off the Rías Baixas (NW Spain) during the upwelling season. *Journal of Geophysical*
746 *Research* 98, 14447–14455, 1993.

747

748 Alvarez-Salgado, X. A., Figueiras, F. G., Villarino, M. L., and Pazos, Y.:
749 Hydrodynamic and chemical conditions during onset of a red-tide assemblage in an
750 estuarine upwelling ecosystem, *Marine Biology*, 130, 509–519, 1998.

751

752 Alvarez, M., Fernández, E., and Pérez, F. F.: Air-sea CO₂ fluxes in a coastal embayment
753 affected by upwelling: physical versus biological control, *Oceanologica Acta*, 22, 5,
754 499–515, 1999.

755

756 Álvarez-Salgado, X. A., Doval, M.D., Borges, A.V, Joint, I., Frankignoulle, M.,
757 Woodward, E.M.S., and Figueiras, F.G.: Off-shelf fluxes of labile materials by an
758 upwelling filament in the NW Iberian Upwelling System, *Prog. Oceanogr.*, 51(2–4),
759 321–337, 2001.

760

761 Álvarez-Salgado, X. A., Beloso, X., Joint, I., Nogueira, E., Chou, L., Pérez, F. F.,
762 Groom, S., Cabanas, J. M., Rees, A.P., and Elskens, M.: New Production of the NW
763 Iberian Shelf during the Upwelling Season over the period 1982-1999. *Deep-Sea Res.*
764 49(10), [http://dx.doi.org/10.1016/S0967-0637\(02\)00094-8](http://dx.doi.org/10.1016/S0967-0637(02)00094-8), 2002.

765

766 Álvarez- Salgado, X. A., Figueiras, F. G., Pérez, F. F., Groom, S., Nogueira, E., Borges,
767 A. V., Chou, L., Castro, C. G., Moncoiffé, G., Ríos, A. F., Miller, A.E.J., Frankignoulle,
768 M., Savidge, G., and Wollast, R.: The Portugal coastal counter current off NW Spain
769 new insights on its biogeochemical variability, *Progress in Oceanography*, 56(2)
770 [http://dx.doi.org/10.1016/S0079-6611\(03\)00007-7](http://dx.doi.org/10.1016/S0079-6611(03)00007-7), 2003.

771

772 Álvarez-Salgado, X. A., Nieto-Cid, M., Piedracoba, S., Crespo, B. G., Gago, J., Brea,
773 S., Teixeira, I. G., Figueiras, F. G., Garrido, J. L., Rosón, G., Castro, C. G., and Gilcoto,
774 M.: Origin and fate of a bloom of *Skeletonema costatum* during a winter
775 upwelling/downwelling sequence in the Ría de Vigo (NW Spain), *Journal of Marine*
776 *Research*, 63, 6, 1127–1149, <http://dx.doi.org/10.1357/002224005775247616>, 2005.

777

778 Alvarez-Salgado, X. A., Nieto-Cid, M., Gago, J., Brea, S., Castro, C. G., Doval, M., and
779 Pérez, F. F.: Stoichiometry of the degradation of dissolved and particulate biogenic
780 organic matter in the NW Iberian upwelling, *Journal of Geophysical Research*, 111,
781 C07017, <http://dx.doi.org/10.1029/2004JC002473>, 2006.

782

783 Anderson, L.: Correction of reversing thermometers and related depth calculations in
784 Baltic water, *Meddelande fran Havsfiskelaboratoriet. Lysekil*, 166, 1974.

785

786 Andersson, A. J., and Mackenzie, F. T.: Revisiting four scientific debates in ocean
787 acidification research, *Biogeosciences*, 9, 893–905, [ww.biogeosciences.net/9/893/2012/](http://www.biogeosciences.net/9/893/2012/),
788 2012.

789

790 Arístegui J., Barton, E. D., Tett, P., Montero, M. F., García-Muñoz, M., Basterretxea,
791 G., Cussatlegras, A. S., Ojeda, A., and de Armas, D.: Variability in plankton community
792 structure, metabolism, and vertical carbon fluxes along an upwelling filament (Cape
793 Juby, NW Africa), *Prog. Oceanogr.*, 62 (2-4), 95–113, 2004.

794

795 Bakun, A., Field, D. B., Redondo-Rodriguez, A., and Weeks, S. J.: Greenhouse gas,
796 upwelling favorable winds, and the future of coastal ocean upwelling ecosystems.
797 *Global Change Biology*, 16, 4, 1213–1228, [https://doi.org/10.1111/j.1365-](https://doi.org/10.1111/j.1365-2486.2009.02094.x)
798 [2486.2009.02094.x](https://doi.org/10.1111/j.1365-2486.2009.02094.x), 2010.

799

800 Barnes, H.: *Apparatus and methods of oceanography. Part one: Chemical*, Allen and
801 Unwin. London, 335 p., 1959.

802

803 Barton, E. D., Largier, J. L., Torres, R., Sheridan, M., Trasviña, A., Souza A., Pazos,
804 Y., and Valle-Levinson, A.: Coastal upwelling and downwelling forcing of circulation
805 in a semi-enclosed bay: Ria de Vigo, *Progress in Oceanography*, 134, 173–189.
806 <https://doi.org/10.1016/j.pocean.2015.01.014>, 2015.

807

808 Barton, E. D., Torres, R., Figueiras, F. G., Gilcoto, M., and Largier, J.: Surface water
809 subduction during a downwelling event in a semienclosed bay, *Journal Geophys.*
810 *Research*, 121, 7088–7107, <https://doi.org/10.1002/2016JC011950>, 2016.

811

812 Barton, E. D., Castro, C. G., Alonso-Pérez, F., Zúñiga, D., Rellán, T., Arbones, B.,
813 Castaño, M., Gilcoto, M., Torres, R., Figueiras, F. G., Pérez, F. F. and Ríos, A. F.: Cria
814 surveys: hydrographic and chemical data, Digital.CSIC,
815 <http://dx.doi.org/10.20350/digitalCSIC/9931>, 2019.
816

817 Bates, N. R., Astor, Y. M., Church, M. J., Currie, K., Dore, J. E., González-Dávila, M.,
818 Lorenzoni, L., Muller-Karger, F., Olafsson, J., and Santana-Casiano, J. M.: A Time-
819 Series View of Changing Surface Ocean Chemistry Due to Ocean Uptake of
820 Anthropogenic CO₂ and Ocean Acidification, *Oceanography*, 27, 1, SPECIAL ISSUE
821 ON Changing Ocean Chemistry, pp. 126–141, Published by: Oceanography Society
822 <https://www.jstor.org/stable/24862128>. 2014.
823

824 Benson, B. B., and Krause, D. J.: The concentration and isotopic fractionation of
825 oxygen dissolved in fresh water and seawater in equilibrium with the atmosphere.
826 *Limnology and Oceanography*, 29(3), 620–632, 1984.
827

828 Blanton, J. O., Atkinson, L. P., Fernandez de Castillejo, F., and Lavin Montero, A.:
829 Coastal upwelling off the Rias Bajas, Galicia, Northwest Spain, I: Hydrography studies.
830 *Rapports et Proc-verbeaux Reun. Cons. into Explor. Mer*, 183, 79–90, 1984.
831

832 Bode, A., Alvarez-Ossorio, M. T., Cabanas, J. M.: Miranda, A., Varela, M.: Recent
833 trends in plankton and upwelling intensity off Galicia (NW Spain), *Progress in*
834 *Oceanography*, 83, 342–350, 2009.
835

836 Caldeira, K., and Wickett, M.E.: Oceanography: anthropogenic carbon and ocean
837 pH, *Nature*, 425, 365, <https://doi.org/10.1038/425365a>, 2003.
838

839 Castro, C. G., Pérez, F. F., Álvarez-Salgado, X. A., Rosón, G., and Ríos, A. F.:
840 Hydrographic conditions associated with the relaxation of an upwelling event off the
841 Galician coast (NW Spain), *Journal of Geophysical Research*, 99, C3, 5135–5147,
842 <https://agupubs.onlinelibrary.wiley.com/doi/10.1029/93JC02735>, 1994.
843

844 Castro, C. G., Nieto-Cid, M., Álvarez-Salgado, X. A., and Pérez, F. F.: Local
845 remineralization patterns in the mesopelagic zone of the ENAW, *Deep Sea Research*
846 Part I, 53 (12), 1925–1940, <http://dx.doi.org/10.1016/j.dsr.2006.09.002>, 2006.

847

848 Castro, C. G., Álvarez-Salgado, X. A., Nogueira, E., Gago, J., Pérez, F. F., Bode, A.,
849 Ríos, A. F., Rosón, G., and Varela, M.: Evidencias bioquímicas do cambio
850 climático. Edita: Xunta de Galicia. Consellería de Medio Ambiente e Desenvolvemento
851 Sostible, *Evidencias e impactos do cambio climático en Galicia*, 303–326, 2009.

852

853 Clayton, T. D., and Byrne, R. H.: Spectrophotometric seawater pH measurements: total
854 hydrogen ion concentration scale calibration of m-cresol purple and at-sea results, *Deep*
855 *Sea Research I*, 40, 10, 2115–2129, [https://doi.org/10.1016/0967-0637\(93\)90048-8](https://doi.org/10.1016/0967-0637(93)90048-8),
856 1993.

857

858 Cobo-Viveros, A. M., Padin, X. A., Otero, P., de la Paz, M., Ruiz-Villareal, M., Ríos,
859 A. F., Pérez, F. F.: Short-term variability of surface carbon dioxide and sea-air CO₂
860 fluxes in the shelf waters of the Galician coastal upwelling system, *Scientia Marina*,
861 77S1, doi: 10.3989/scimar.03733.27C, 2013.

862

863 Culberson, C. H., Knapp, G., Stalcup, M. C., Williams, R. T., and Zemlyak, F.: A
864 comparison of methods for the determination of dissolved oxygen in seawater. WOCE
865 Report 73/91, 77 pp, 1991.

866

867 DelValls, T. A., and Dickson, A. G.: The pH of buffers based on 2-amino-2-
868 hydroxymethyl-1,3-propanediol (“tris”) in synthetic sea water, *Deep-Sea Res. I*, 45,
869 1541–1554, 1998.

870

871 Dickson, A.G., Sabine, C.L., and Christian, J.R.: Guide to best practices for ocean CO₂
872 measurements. PICES Special Publication 3, 191 pp, 2007.

873

874 Doval, M., Nogueira, E., and Pérez, F. F.: Spatio-temporal variability of the
875 thermohaline and biogeochemical properties and dissolved organic carbon in a coastal
876 embayment affected by upwelling: the Ría de Vigo (NW Spain). *Journal of Marine*
877 *Systems*, 14, 1-2, 135–150, [https://doi.org/10.1016/S0924-7963\(97\)80256-4](https://doi.org/10.1016/S0924-7963(97)80256-4), 1998.

878

879 Doval, M. D., Alvarez-Salgado, X. A., and Perez, F. F.: Dissolved organic carbon in a
880 temperate embayment affected by coastal upwelling, *Mar. Ecol. Prog. Ser.*, 157, 21–37,
881 doi:10.3354/meps157021, 1997a.

882

883 Doval, M. D., Fraga, F. and Perez, F.F.: Determination of dissolved organic nitrogen in
884 seawater using Kjeldahl digestion after inorganic nitrogen removal, *Oceanol. Acta.*
885 <https://archimer.ifremer.fr/doc/00093/20429/18096.pdf>, 1997b.

886

887 Doval, M.D., López, A., and Madriñán, M.: Temporal variation and trends of inorganic
888 nutrients in the coastal upwelling of the NW Spain (Atlantic Galician rías),
889 *Journal of Sea Research*, 108, 19–29, <https://doi.org/10.1016/j.seares.2015.12.006>,
890 2016.

891

892 Fraga F.: Upwelling off the Galician coast, northwest Spain. *Coastal Upwelling*,
893 American Geophysical Union, Washington DC, pp. 176–182,
894 <https://doi.org/10.1029/CO001p0176>, 1981.

895

896 Fraga, F., Mouriño, C., and Manriquez, M.: Las masas de agua en la costa de Galicia:
897 junio-octubre. *Result. Exped. Cient. Supl. Invest. Pesq.*, 10, 51–77,
898 <http://hdl.handle.net/10261/90380>, 1982.

899

900 Fraga, F., Pérez, F. F., Figueiras, F. G., and Ríos, A. F.: Stoichiometric variations of N,
901 P, C and O₂ during a *Gymnodinium catenatum* red tide and their interpretation, *Marine*
902 *Ecology Progress Series*, 87, 1-2, 123–134, doi:10.3354/meps087123, 1992.

903

904 Figueiras, F. G., Jones, K., Mosquera, A. M., Álvarez Salgado, X. A., Edwards, A. and
905 MacDougall, N.: Red tide assemblage formation in an estuarine upwelling ecosystem:
906 Ria de Vigo, *Journal of Plankton Research*, 16 (7), 857–878,
907 <https://doi.org/10.1093/plankt/16.7.857>, 1994.

908

909 Froján, M., Arbones, B., Zúñiga, D., Castro, C. G., and Figueiras, F. G.: Microbial
910 plankton community in the Ría de Vigo (NW Iberian upwelling system): impact of the

911 culture of *Mytilus galloprovincialis*, *Mar Ecol Prog Ser*, 498, 43–54,
912 <https://doi.org/10.3354/meps10612>, 2014.

913

914 Froján, M., Figueiras, F. G., Zúñiga, D., Alonso-Pérez, F., Arbones, B., and Castro, C.
915 G.: Influence of Mussel Culture on the Vertical Export of Phytoplankton Carbon in a
916 Coastal Upwelling Embayment (Ría de Vigo, NW Iberia), *Estuaries and Coasts*, 39,
917 1449–1462, <https://doi.org/10.1007/s12237-016-0093-1>, 2016.

918

919 Froján, M., Castro, C. G., Zúñiga, D., Arbones, A., Alonso-Pérez, F., and Figueiras, F.
920 G.: Mussel farming impact on pelagic production and respiration rates in a coastal
921 upwelling embayment (Ría de Vigo, NW Spain), *Estuarine, Coastal and Shelf Science*,
922 204, 130–139, <https://doi.org/10.1016/j.ecss.2018.02.025>, 2018.

923

924 Frouin, R., Fiúza, A. F. G., Ambar, I., and Boyd, T. J.: Observations of a poleward
925 surface current off the coasts of Portugal and Spain during winter, *Journal of*
926 *Geophysical Research*, 95, 679–691, 1990.

927

928 Feely, R. A., Sabine, C. L., Hernandez-Ayon, J. M., Ianson, D., and Hales, B: Evidence
929 for upwelling of corrosive “acidified” water onto the continental shelf, *Science*
930 320(5882), 1490–1492, doi:10.1126/science.1155676, 2008.

931

932 Gago, J., Alvarez-Salgado, X. A., Gilcoto, M., and Pérez, F. F.: Assessing the
933 contrasting fate of dissolved and suspended organic carbon in a coastal upwelling
934 system (Ría de Vigo, NW Iberian Peninsula), *Estuarine, Coastal and Shelf Science*, 56,
935 2, 271–279, [http://dx.doi.org/10.1016/S0272-7714\(02\)00186-5](http://dx.doi.org/10.1016/S0272-7714(02)00186-5), 2003a.

936

937 Gago, J., Alvarez-Salgado, X. A., Pérez, F. F., and Ríos, A. F.: Partitioning of physical
938 and biogeochemical contributions to short-term variability of pCO₂ in a coastal
939 upwelling system a quantitative approach, *Marine Ecology Progress*, 255, 43–54,
940 <http://dx.doi.org/10.3354/meps25504>, 2003b.

941

942 Gago, J., Gilcoto, M., Pérez, F. F., and Ríos, A.F.: Short-term variability of fCO₂ in
943 seawater and air-sea CO₂ fluxes, *Marine Chemistry*, 80, 4, 247–264,
944 [http://dx.doi.org/10.1016/S0304-4203\(02\)00117-2](http://dx.doi.org/10.1016/S0304-4203(02)00117-2), 2003c.

945

946 Gilcoto, M., Largier, J. L., Barton, E. D., Piedracoba, S., Torres, R., Graña, R., Alonso-
947 Pérez, F., Villacieros-Robineau, N., and de la Granda, F.: Rapid response to coastal
948 upwelling in a semienclosed bay, *Geophysical Research Letters*, 44(5), 2388–2397, doi:
949 10.1002/2016GL072416, 2017.

950

951 González-Pola, C., Lavín, A., Vargas-Yáñez, M.: Intense warming and salinity
952 modification of intermediate water masses in the southeastern corner of the Bay of
953 Biscay for the period 1992–2003, *Journal of Geophysical Research*, 110, C05020,
954 doi:10.1029/2004JC002367, 2005.

955

956 Grasshoff, K., Johannsen, H.: A New Sensitive and Direct Method for the Automatic
957 Determination of Ammonia in Sea Water, *ICES Journal of Marine Science*, 34(3), 516–
958 521, <https://doi.org/10.1093/icesjms/34.3.516>, 1972.

959

960 Grasshoff, K., Ehrhardt, M., Kremling, K.: *Methods of Seawater Analysis*, 2nd. ed.
961 Verlag Chemie, Weinheim, 419 pp, 1983.

962

963 Gruber, N., Hauri, C., Lachkar, Z., Loher, D., Frolicher, T. L., and Plattner, G. K.:
964 Rapid progression of ocean acidification in the California Current System, *Science*, 337,
965 220–223, doi:10.1126/science.1216773, 2012.

966

967 Harvey, J.: θ -S relationship and water masses in the eastern North Atlantic. *Deep-Sea*
968 *Research*, 29, 1021-1033, 1982.

969

970 Hauri, C., Gruber, N., Plattner, G. K., Alin, S., Feely, R. A., Hales, B., and Wheeler,
971 P. A.: Ocean acidification in the California Current System, *Oceanography*, 22, 58–69,
972 doi:10.5670/oceanog.2009.97, 2009.

973

974 Hauri, C., Gruber, N., Vogt, M. S., Doney, C., Feely, R. A., Lachkar, Z., Leinweber, A.,
975 McDonnell, A. M. P., Munnich, M., and Plattner, G.K.: Spatiotemporal variability and
976 long-term trends of ocean acidification in the California Current System,
977 *Biogeosciences*, 10, 193–216, doi:10.5194/bg-10-193-2013, 2013.

978 Hofmann, G. E.: High-frequency dynamics of ocean pH: A multi-ecosystem
979 comparison, PLoS One, 6(12), e28983, doi:10.1371/journal.pone.0028983, 2011.
980

981 IPCC: Climate Change 2013: the physical science basis Contribution of Working Group
982 I to the Fifth Assessment Report of the Intergovernmental Panel on Climate Change ed
983 T F Stocker et al (Cambridge: Cambridge University Press) pp 1535,
984 www.ipcc.ch/report/ar5/wg1/, 2013.
985

986 Lachkar, Z.: Effects of upwelling increase on ocean acidification in the California and
987 Canary Current systems, Geophys. Res. Lett., 41, 90–95, doi:10.1002/2013GL058726,
988 2014.
989

990 Lassoued. J., Babarro, J., Padín, X. A., Comeau, L., Bejaoui, N., and Pérez, F.:
991 Behavioural and eco-physiological responses of the mussel *Mytilus galloprovincialis*
992 to acidification and distinct feeding regimes, Marine Ecology Progress Series, 626, 97–
993 108, doi: 10.3354/meps13075, 2019.
994

995 Lauvset, S.K., and Gruber, N.: Long-term trends in surface ocean pH in the North
996 Atlantic, Marine Chemistry, 162, 71–76,
997 <https://doi.org/10.1016/j.marchem.2014.03.009>, 2014.
998

999 Lauvset, S. K., Gruber, N., Landschützer, P., Olsen, A., and Tjiputra, J.: Trends and
1000 drivers in global surface ocean pH over the past 3 decades, Biogeosciences, 12(5),
1001 1285–1298, doi:10.5194/bg-12-1285-2015, 2015.
1002

1003 Lewis, E., Wallace, D.W.R.: Program developed for CO₂ system calculations,
1004 ORNL/CDIAC-105, Carbon Dioxide Information Analysis Center, Oak Ridge National
1005 Laboratory, Oak Ridge, TN, USA, 1998.
1006

1007 Lemos, R. T., and Sansó, B.: Spatio-temporal variability of ocean temperature in
1008 the Portugal Current System, Journal of Geophysical Research, 111, C04010,
1009 doi:10.1029/2005JC003051, 2006.
1010

1011 Lueker, T. J., Dickson, A. G., and Keeling, C. D.: Ocean pCO₂ calculated from
1012 dissolved inorganic carbon, alkalinity, and equations for K-1 and K-2: validation based
1013 on laboratory measurements of CO₂ in gas and seawater at equilibrium, *Mar. Chem.*,
1014 70, 105–119, 2000.
1015

1016 McElhany, P. and Shallin Busch, D.: Appropriate pCO₂ treatments in ocean
1017 acidification experiments, *Marine Biology*, 160, 1807–1812,
1018 <https://doi.org/10.1007/s00227-012-2052-0>, 2013.
1019

1020 Mehrbach, C., Culberson, C. H., Hawley, J. E., and Pytlowicz, R. M.: Measurements of
1021 the apparent dissociation constant of carbonic acid in seawater at atmospheric pressure,
1022 *Limnology and Oceanography*, 18, 897–907, 1973.
1023

1024 Miguez, B. M., Fariña-Busto, L., Figueiras, F. G., Pérez, F. F.: Succession of
1025 phytoplankton assemblages in relation to estuarine hydrodynamics in the Ria de Vigo,
1026 *Scientia Marina*, 65, S1, <https://doi.org/10.3989/scimar.2001.65s165>, 2001.
1027

1028 Mouriño, C., and Fraga, F.: Determinación de nitratos en agua de mar, *Investigaciones*
1029 *Marinas*, 49 (1), 81–96, 1985.
1030

1031 Nieto-Cid, M., Alvarez-Salgado, X. A., Brea, S., and Pérez, F. F.: Cycling of dissolved
1032 and particulate carbohydrates in a coastal upwelling system (NW Iberian Peninsula),
1033 [doi:10.3354/meps283039](https://doi.org/10.3354/meps283039), 2004.
1034

1035 Nieto-Cid, M., Alvarez-Salgado, X. A., and Pérez, F. F.: Microbial and photochemical
1036 reactivity of fluorescent dissolved organic matter in a coastal upwelling system
1037 <https://doi.org/10.4319/lo.2006.51.3.1391>, 2006.
1038

1039 Nogueira, E., Pérez, F. F., and Ríos, A. F.: Seasonal and long-term trends in an
1040 estuarine upwelling ecosystem (Ría de Vigo, NW Spain), *Estuarine, Coastal and Shelf*
1041 *Science* 44, 285–300, 1997.
1042

1043 Olsen, A., Lange, N., Key, R. M., Tanhua, T., Álvarez, M., Becker, S., et al.:
1044 GLODAPv2.2019: An update of GLODAPv2. *Earth System Science Data*, 11(3), 1437-
1045 1461. <https://doi.org/10.5194/essd-11-437-2019>, 2019.
1046
1047 Orr, F. M.: Onshore Geologic Storage of CO₂, *Science*, 25, 325, 1656–1658, doi:
1048 10.1126/science.1175677, 2009.
1049
1050 Otero, P., Ruiz-Villarreal, M., and Peliz, A.: Variability of river plumes off Northwest
1051 Iberia in response to wind events, *Journal of Marine Systems*, 72(1-4), 238–255, 2008.
1052
1053 Padin X. A., Castro, C. G., Ríos, A.F., and Pérez, F.F.: Oceanic CO₂ uptake and
1054 biogeochemical variability during the formation of the Eastern North Atlantic Central
1055 water under two contrasting NAO scenarios, *Journal of Marine Systems*, 84, 3-4, 96–
1056 105, <https://doi.org/10.1016/j.jmarsys.2010.10.002>, 2010.
1057
1058 Pauly, D., and Christensen, V.: Primary production required to sustain global fisheries,
1059 *Nature*, 374(6519), 255–257, 1995.
1060
1061 Pérez, F. F., and Fraga, F.: A precise and rapid analytical procedure for alkalinity
1062 determination, *Marine Chemistry*, 21, 169–182, 1987a.
1063
1064 Pérez, F. F., and Fraga, F.: The pH measurements, in seawater on the NBS scale,
1065 *Marine Chemistry*, 21, 315–327, 1987b.
1066
1067 Pérez, F. F., Rios, A. F., and Rosón, G.: Sea surface carbon dioxide off the Iberian
1068 Peninsula North Eastern Atlantic Ocean, *Journal of Marine Systems*, 19, 27–46, 1999.
1069
1070 Perez, F. F., Alvarez-Salgado, X. A., and Rosón G.: Stoichiometry of the net ecosystem
1071 metabolism in a coastal inlet affected by upwelling. The Ría de H (NW Spain), *Marine*
1072 *Chemistry*, 69, 3-4, 217–236, 2000.
1073
1074 Pérez, F. F., Padin, X. A., Pazos, Y., Gilcoto, M., Cabanas, M., Pardo, P. C., Doval, M.,
1075 D., and Farina-Busto, L.: Plankton response to weakening of the Iberian coastal
1076 upwelling. *Global Change Biology*, 16(4), 1258–1267, 2010.

1077

1078 Pérez, F. F., Velo, A., Padin, X. A., Doval, M. D., Prego, R.: ARIOS DATABASE: An
1079 Acidification Ocean Database for the Galician Upwelling Ecosystem,
1080 Instituto de Investigaciones Marinas, Consejo Superior de Investigaciones Cientificas
1081 (CSIC), doi: 10.20350/digitalCSIC/12498, 2020.

1082

1083 Piedracoba, S., Alvarez-Salgado, X. A., Rosón G., and Herrera, J. L.: Short timescale
1084 thermohaline variability and residual circulation in the central segment of the coastal
1085 upwelling system of the Ría de Vigo (northwest Spain) during four contrasting periods,
1086 <https://doi.org/10.1029/2004JC002556>, 2005.

1087

1088 Prego, R., Fraga, F., and Rios, A. F.: Water interchange between the Ria of Vigo and
1089 the continental shelf. *Scientia Marina* 54, 95–100, 1990.

1090

1091 Raven, J., Caldeira, K., Elderfield, H., Hoegh-Guldberg, O., Liss, P., Riebesell, U.,
1092 Sphepherd, J., Turley, C., and Watson, A.: Ocean acidification due to increasing
1093 atmospheric carbon dioxide: Royal Society Policy Document 12/05, 68 p, 2005.

1094

1095 Rios, A. F., Pérez, F. F., and Fraga, F.: Water masses in the upper and middle North
1096 Atlantic Ocean east of the Azores, *Deep-Sea Res. Part I*, 39, 645–658, 1992.

1097

1098 Rosón, G., Pérez, F. F., Alvarez-Salgado, X. A., and Figueiras, F. G.: Variation of both
1099 thermohaline and chemical properties in an estuarine upwelling ecosystem -Ría de
1100 Arousa. 1. Time evolution, *Estuarine Coastal and Shelf Science*, 41, 2, 195–213, doi
1101 10.1006/ecss.1995.0061, 1995.

1102

1103 Rosón, G., Cabanas, J. M., Pérez, F. F., Herrera, J. L., Ruiz-Villarreal, M., Castro, C.
1104 G., Piedracoba, S., and Álvarez-Salgado, X. A.: Evidencias do cambio climático na
1105 Hidrografía e a dinámica das Rías e da plataforma galega. Edita: Xunta de Galicia.
1106 Consellería de Medio Ambiente e Desenvolvemento Sostible, *Evidencias e impactos do*
1107 *cambio climático en Galicia*, 287-302, 2009.

1108

1109 Sabine, C. L., Feely, R. A., Gruber, N., Key, R. M., Lee, K., Bullister, J. L.,
1110 Wanninkhof, R., Wong, C. S., Wallace, D. W. R., Tilbrook, B., Millero, F. J., Peng, T.-

1111 H., Kozyr, A., Ono, T., and Rios, A. F.: The oceanic sink for anthropogenic CO₂.
1112 Science 305, 367–371, 2004.
1113

1114 Sarmiento, J. L., and Gruber, N.: Ocean biogeochemical dynamics. Princeton Univ.
1115 Press. 2006.
1116

1117 Souto, C., Gilcoto, M., Fariña-Busto, L., and Pérez, F. F.: Modeling the residual
1118 circulation of a coastal embayment affected by wind-driven upwelling: Circulation of
1119 the Ria de Vigo (NW Spain), Journal of Geophysical Research - Oceans, 108 C11
1120 (3340), doi: 10.1029/2002JC001512, 2003.
1121

1122 SCOR-UNESCO: Determination of Photosynthetic Pigments in Seawater. UNESCO,
1123 Paris, 1966.
1124

1125 Strickland, J. D. H., and Parsons, T.R.: A practical handbook of seawater analysis,
1126 Fisheries Research Board of Canada, Ottawa, Ontario, 1972.
1127

1128 Takeshita, Y., Frieder, C. A., Martz, T. R., Ballard, J. R., Feely, R. A., Kram, S., Nam,
1129 S., Navarro, M. O., Price, N. N., and Smith, J. E.: Including high-frequency variability
1130 in coastal ocean acidification projections, Biogeosciences, 12(19), 5853–5870,
1131 doi:10.5194/bg-12-5853-2015, 2015.
1132

1133 Teira, E., Martínez-García, S., Lonborg, C., and Álvarez-Salgado, X. A.: Growth rates
1134 of different phylogenetic bacterioplankton groups in a coastal upwelling system,
1135 Environmental microbiology reports, 1,6, 545–554, [https://doi.org/10.1111/j.1758-
1136 2229.2009.00079.x](https://doi.org/10.1111/j.1758-2229.2009.00079.x), 2009.
1137

1138 UNESCO: Background papers and supporting data on the Practical Salinity Scale 1978.
1139 UNESCO Tech. Papers in Marine Science, 37, 144pp, 1981.
1140

1141 Uppström, L. R.: Boron = Chlorinity ratio of deep-sea water from Pacific Ocean, Deep-
1142 Sea Res., 21, 161–162, 1974.
1143

1144 Van Heuven, S., Pierrot, D., Rae, J.W.B., Lewis, E., Wallace, D.W.R. MATLAB
1145 Program Developed for CO₂ System Calculations. ORNL/CDIAC-105b. Carbon
1146 Dioxide Information Analysis Center, Oak Ridge National Laboratory, U.S. Department
1147 of Energy, Oak Ridge, Tennessee, 2011.
1148

1149 Velo, A., Pérez, F.F., Lin, X., Key, R.M., Tanhua, T., de la Paz, M., Olsen, A., van
1150 Heuven, S., Jutterström, S., Ríos, A.F.: CARINA data synthesis project: pH data scale
1151 unification and cruise adjustments, *Earth Syst. Sci. Data*, 2, 133–155, doi:10.5194/essd-
1152 2-133-2010, 2010.
1153

1154 Velo, A., Cacabelos, J., Pérez, F.F., Ríos, A.F.: GO-SHIP Software and Manuals:
1155 Software packages and best practice manuals and knowledge transfer for sustained
1156 quality control of hydrographic sections in the Atlantic. (Version v1.0.0), Zenodo,
1157 <http://doi.org/10.5281/zenodo.2603122>, 2019.
1158

1159 Villaceros-Robineau, N., Zúñiga, D., Barreiro-González, B., Alonso-Pérez, F.,
1160 de la Granda, F., and Froján, M.: Bottom boundary layer and particle dynamics in an
1161 upwelling affected continental margin (NW Iberia), *Journal of Geophysical Research:*
1162 *Oceans*, 124, <https://doi.org/10.1029/2019JC015619>, 2019.
1163

1164 Wahl, M., Saderne, V., and Sawall, Y.: How good are we at assessing the impact of
1165 ocean acidification in coastal systems? Limitations, omissions and strengths of
1166 commonly used experimental approaches with special emphasis on the neglected role of
1167 fluctuations, *Mar. Freshw. Res.*, 67, 25–36, doi:10.1071/MF14154, 2016.
1168

1169 Wolf-Gladrow, D. A., Riebesell, U., Burkhardt, S., and Bijma, J.: Direct effects of CO₂
1170 concentration on growth and isotopic composition of marine plankton, *Tellus*, 51B, 461,
1171 1999.
1172

1173 Wooster, W. S., Bakun, A., and McClain, D. R.: The seasonal upwelling cycle along the
1174 eastern boundary of the North Atlantic, *Journal of Marine Research*, 34, 131–141, 1976.
1175

1176 Zúñiga, D., Villaceros-Robineau, N., Salgueiro, E., Alonso-Pérez, F., Rosón, G.,
1177 Abrantes, F., and Castro, C. G.: Particle fluxes in the NW Iberian coastal upwelling

1178 system: Hydrodynamical and biological control. *Continental Shelf Research*, 123
1179 (2016), 89–98, <http://dx.doi.org/10.1016/j.csr.2016.04.008>, 2016.

1180

1181 Zúñiga, D., Santos, C., Froján, M., Salgueiro, E., Rufino, M. M., de la Granda, F.,
1182 Figueiras, F. G., Castro, C. G., and Abrantes, F.: Diatoms as a paleoproductivity proxy
1183 in the NW Iberian coastal upwelling system (NE Atlantic), *Biogeosciences*, 14, 1165–
1184 1179, www.biogeosciences.net/14/1165/2017, 2017.

1185

1186

1187

1188

1189

1190

1191

1192

1193

1194

1195

1196

1197

1198

1199

1200

1201

1202

1203

1204

1205

1206

1207

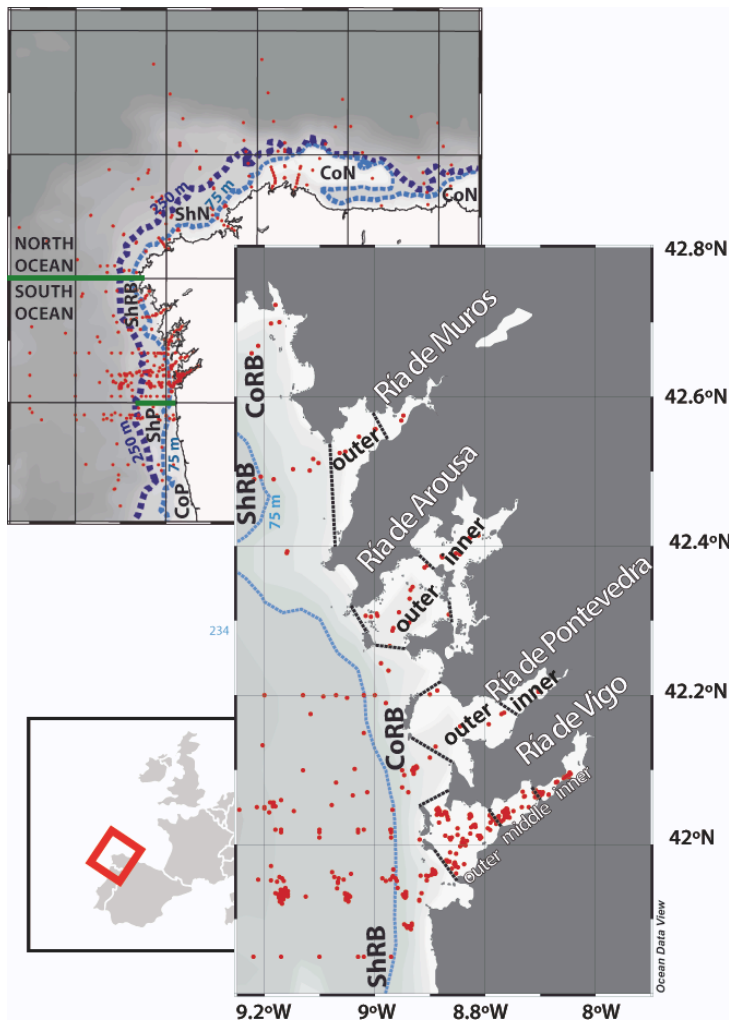
1208

1209

1210

1211

1212



1213

1214

1215 Figure 1. Map of all stations (red dots) including the geographical areas selected to
1216 classify the ARIOS database from isobath of 250 m (dark blue line) and 75 metres (light
1217 blue line), latitudinal criterion (green lines) and geographical lines (black lines).

1218

1219

1220

1221

1222

1223

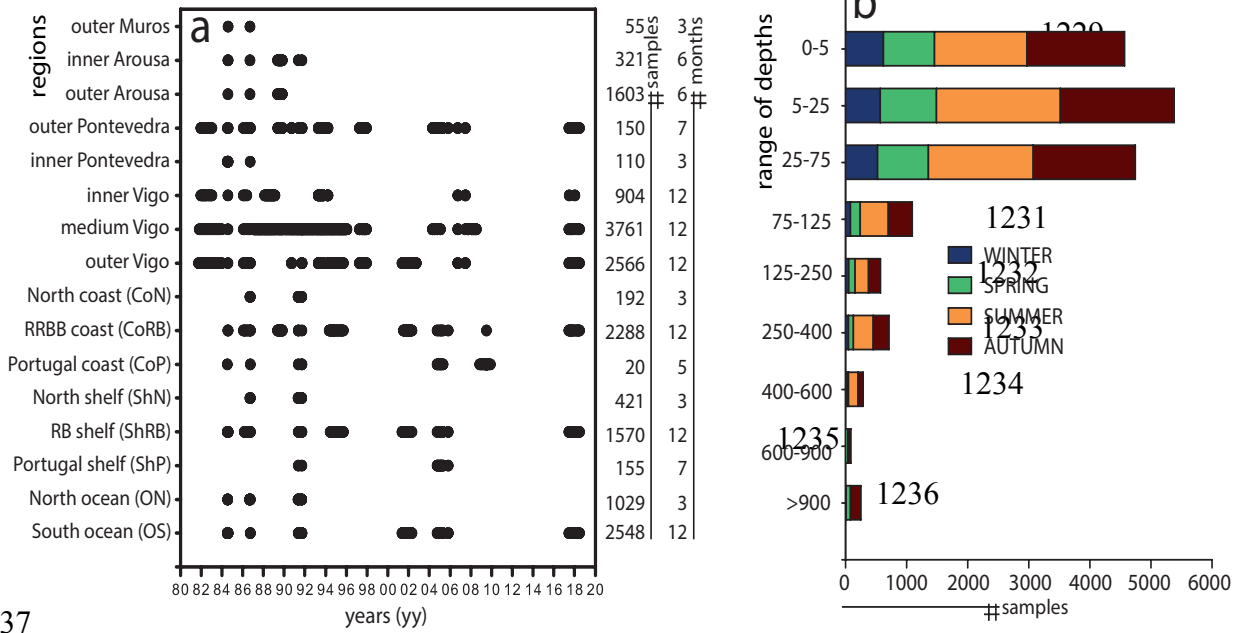
1224

1225

1226

1227

1228



1237

1238 Figure 2. a) Temporal distribution of the observations in the geographical boxes
 1239 included in the ARIOS dataset. b) Seasonal distribution of the measurements in relation
 1240 to depth.

1241

1242

1243

1244

1245

1246

1247

1248

1249

1250

1251

1252

1253

1254

1255

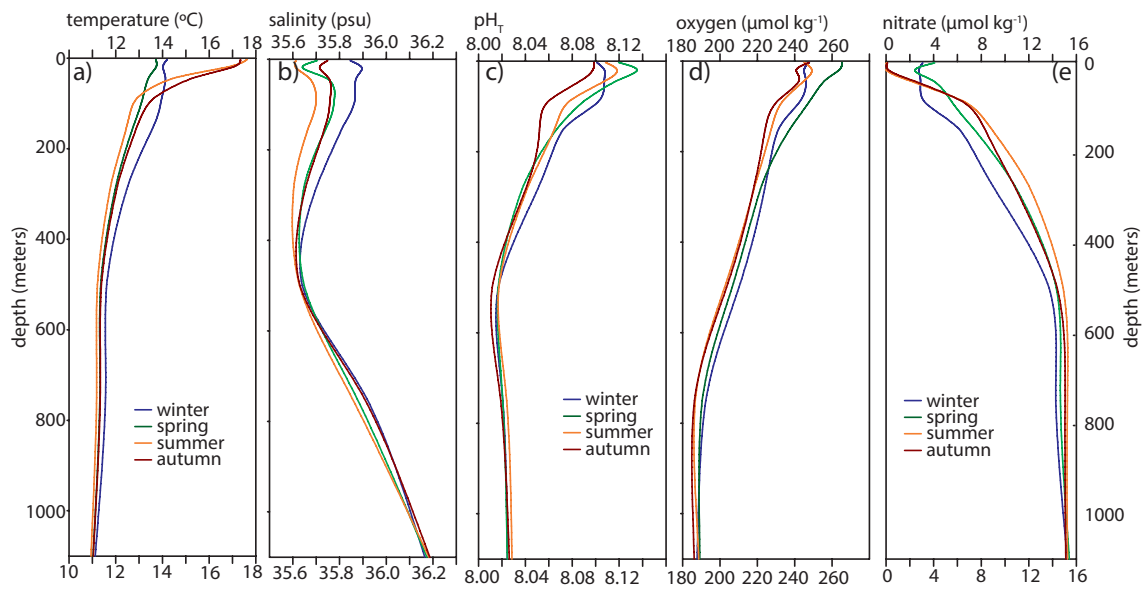
1256

1257

1258

1259

1260



1261

1262

1263 Figure 3. Profiles of seasonal means of temperature (a), salinity (b), pH_T (c), oxygen (d)
1264 and nitrate concentration (e) in the first 1100 meters of the region South Ocean shown
1265 in Fig. 1.

1266

1267

1268

1269

1270

1271

1272

1273

1274

1275

1276

1277

1278

1279

1280

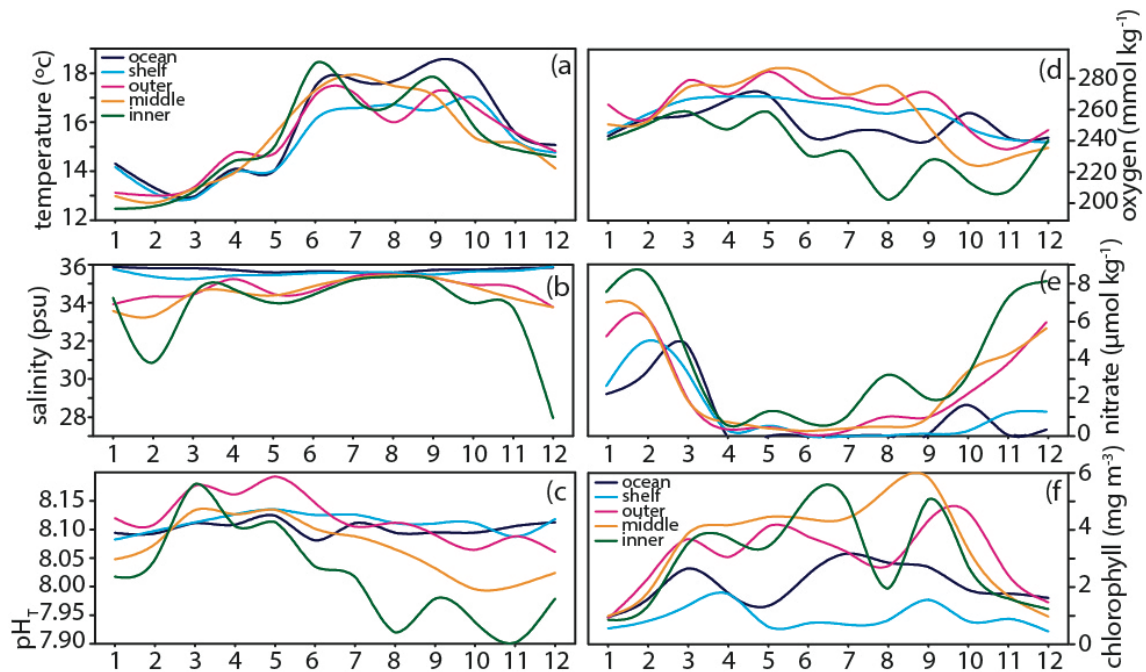
1281

1282

1283

1284

1285



1286

1287

1288 Figure 4. Sea surface (<5 meters depth) seasonal cycles in 1976 - 2018 of temperature
1289 (a), salinity (b), pH_T (c), oxygen concentration (d), nitrate concentration (e) and
1290 chlorophyll (f) at sea surface for five geographical boxes shown in Fig. 1: South Ocean,
1291 RB shelf and outer, middle and inner Ria de Vigo for the entire period of the ARIOS
1292 database.

1293

1294

1295

1296

1297

1298

1299

1300

1301

1302

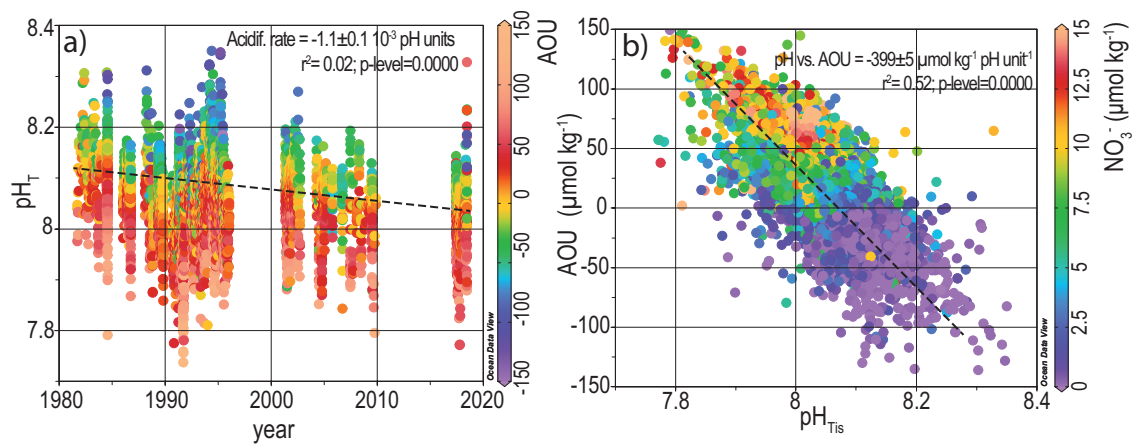
1303

1304

1305

1306

1307



1308

1309 Figure 5. Time-series of pH ARIOS data. The black line depicts the long-term trend.

1310 Scatter diagram of AOU vs pH_T including the nitrate concentration shown as colour of
1311 every dot.

1312

1313

1314

1315

1316

1317

1318

1319

1320

1321

1322

1323

1324

1325

1326

1327

1328

1329

1330

1331

1332

1333 Table 1. Discrete measurements of projects gathered in the ARIOS database and
1334 associated information: including dates, the number of days between the start and the
1335 end of sampling period (#d), sample number (#), the principal investigator (PI),
1336 measured parameters, link to data repository and the sampled geographical area.
1337
1338 - All projects include measurements of *T*, *S*. Others as *pH*, alkalinity (*Alk*), nutrient
1339 (*Nut*), oxygen (*O₂*) concentration, chlorophyll (*Chla*) are indicated.
1340 - The concentration units of these variables are $\mu\text{mol kg}^{-1}$ or $\mu\text{mol L}^{-1}$ (*) and the *pH*
1341 measurements in NBS scale (°) or in total scale.
1342 - Regions are identified as ocean (*O*), shelf (*Sh*), coastal (*Co*), Ría de Vigo (*RV*), Ría de
1343 Pontevedra (*RP*), Ría de Arousa (*RA*) and Ría de Muros (*RM*) while the superscript
1344 index means south (^{*S*}), north (^{*N*}), Portugal (^{*P*}), Rías Baixas (^{*RB*}), outer (^{*O*}), middle (^{*M*})
1345 and inner (^{*I*}).
1346
1347
1348
1349
1350
1351
1352
1353
1354
1355
1356
1357
1358
1359
1360
1361
1362
1363
1364
1365
1366

| EXPOCODE | PROJECT | DATE | #d | IP | # | CTD | O ₂ | Nut | pH | Alk | Chla | CRM | Data Repository | REGIONS |
|--------------|------------------|----------|------|---------------|------|-----|----------------|-----|----|-----|------|-----|---|---|
| 29LP19761026 | Ría Vigo 1977 | 26/10/76 | 413 | F Fraga | 135 | N | N | S* | S° | N | N | N | http://dx.doi.org/10.20350/digitalCSIC/9917 | Co ^{RB} |
| 29LP19810929 | Ría Vigo 1981-83 | 29/9/81 | 472 | F Fraga | 748 | N | S* | S* | S° | S | N | N | http://dx.doi.org/10.20350/digitalCSIC/9918 | RV ^{O,M,I} |
| 29LP19830215 | Ría Vigo 1983-84 | 15/2/83 | 322 | F Fraga | 312 | N | S* | S* | S° | S | N | N | http://dx.doi.org/10.20350/digitalCSIC/9919 | RV ^{O,M} |
| 29GD19840711 | GALICIA-VIII | 11/7/84 | 28 | F Fraga | 1865 | N | S | S | S° | S | S | N | http://dx.doi.org/10.20350/digitalCSIC/9908 | O ^{N,S} , Sh ^{RB} , Co ^{P,RB} , RV ^{O,M,I} , RA ^{O,I} , RP ^{O,I} , RM |
| 29GD19860121 | Ría Vigo 1986 | 21/1/86 | 203 | F Fraga | 332 | N | S | S | S° | S | S | N | http://dx.doi.org/10.20350/digitalCSIC/9910 | Sh ^{RB} , Co ^{RB} , RV ^{O,M,I} |
| 29GD19860904 | GALICIA-IX | 23/9/86 | 5 | F Fraga | 1640 | N | S | S | S° | S | S | N | http://dx.doi.org/10.20350/digitalCSIC/9911 | O ^{N,S} , Sh ^{RB,N} , Co ^{P,RB,N} , RV ^{O,M,I} , RA ^{O,I} , RP ^{O,I} , RM |
| 29LP19870120 | PROVIGO | 17/9/87 | 3290 | F F Pérez | 2317 | N | S | S | S° | N | S | N | http://dx.doi.org/10.20350/digitalCSIC/9924 | RV ^M |
| 29LP19880212 | LUNA 88 | 12/2/88 | 367 | A F Rios | 468 | N | S | S | S° | S | S | N | http://dx.doi.org/10.20350/digitalCSIC/9907 | RV ^{M,I} |
| 29IN19890512 | GALICIA-X | 5/5/89 | 171 | F F Pérez | 3113 | N | S | S | S° | S | S | N | http://dx.doi.org/10.20350/digitalCSIC/9920 | Co ^{RB} , RA ^{O,I} |
| 29IN19900914 | Ría Vigo 1990 | 14/9/90 | 13 | FG Figueiras | 108 | Y | S | S | S° | S | S | N | http://dx.doi.org/10.20350/digitalCSIC/9921 | RV ^{O,M,I} |
| 29IN19910510 | GALICIA-XI | 5/5/91 | 4 | F F Pérez | 327 | Y | S | S | S° | S | S | N | http://dx.doi.org/10.20350/digitalCSIC/9922 | O ^{N,S} , Sh ^{P,RB,N} , Co ^{P,RB,N} , RA ^O |
| 29IN19910910 | GALICIA-XII | 15/9/91 | 10 | F G Figueiras | 663 | Y | S | S | S° | S | S | N | http://dx.doi.org/10.20350/digitalCSIC/9923 | O ^{N,S} , Sh ^{P,RB,N} , Co ^{P,RB,N} , RV ^{O,M,I} , RA ^O |
| 29LP19930413 | Ría Vigo 1993-94 | 22/3/94 | 344 | F G Figueiras | 406 | Y | S | S | S° | S | S | N | http://dx.doi.org/10.20350/digitalCSIC/9927 | RV ^{O,M,I} |
| 29JN19940505 | Ría Vigo 1994-95 | 5/5/94 | 504 | M Cabanas | 669 | Y | S | S | S° | S | S | N | http://dx.doi.org/10.20350/digitalCSIC/9926 | Sh ^{RB} , Co ^{RB} , RV ^O |
| 29MY19970407 | CIRCA-97 | 7/4/97 | 248 | F F Pérez | 547 | Y | S | N | S° | S | S | N | http://dx.doi.org/10.20350/digitalCSIC/9928 | RV ^{O,M,I} |
| 29MY20010515 | DYBAGA | 15/5/01 | 344 | F F Pérez | 1421 | Y | S | S* | S | S | S | Y | http://dx.doi.org/10.20350/digitalCSIC/9929 | Sh ^{P,RB} , Co ^{RB} , RV ^O |
| 29MY20010702 | REMODA | 2/7/01 | 451 | X A Alvarez | 203 | Y | S | S* | S | S | S | Y | http://dx.doi.org/10.20350/digitalCSIC/9930 | RV ^O |
| 29MY20040419 | FLUVBE | 19/4/04 | 283 | C G Castro | 187 | Y | S | S* | S | S | S | Y | to be submitted | RV ^{M,I} |
| 29CS20041004 | ZOTRACOS | 4/10/04 | 389 | M Cabanas | 371 | Y | S | S | S | S | S | Y | http://dx.doi.org/10.20350/digitalCSIC/9932 | Sh ^{P,RB} , Co ^{P,RB} , RP ^O |
| 29MY20060926 | CRÍA | 26/9/06 | 275 | D Barton | 197 | Y | S | S* | S | S | S | Y | http://dx.doi.org/10.20350/digitalCSIC/9931 | RV ^{O,M,I} |
| 29MY20070917 | RAFTING | 17/9/07 | 301 | C G Castro | 287 | Y | S | S* | S | S | S | Y | to be submitted | RV ^M |
| 29MY20081105 | LOCO | 5/11/08 | 378 | X A Alvarez | 72 | Y | S | S | S | S | S | Y | http://dx.doi.org/10.20350/digitalCSIC/9936 | Co ^{RB} |
| 29AH20090710 | CAIBEX-I | 16/7/09 | 11 | D Barton | 191 | Y | S | S | S | S | S | Y | http://dx.doi.org/10.20350/digitalCSIC/9934 | Co ^{P,RB} |
| 29MY20170609 | ARIOS | 9/6/17 | 382 | FF Pérez | 1114 | Y | S | S* | S | S | S | Y | http://dx.doi.org/10.20350/digitalCSIC/9963 | Sh ^{P,RB} , Co ^{RB} , RV ^{O,M,I} |

1367

1368

| | SS_{range} | r^2_{ss} | $t_{interannual}$ | r^2 | p-value |
|--------|--------------|------------|-------------------|-------|---------|
| OCEAN | 0.050 | 0.17 | -0.0012±0.0002 | 0.21 | 0.0000 |
| SHELF | 0.050 | 0.06 | -0.0017±0.0003 | 0.15 | 0.0009 |
| OUTER | 0.120 | 0.24 | -0.0027±0.0003 | 0.21 | 0.0000 |
| MIDDLE | 0.130 | 0.28 | -0.0022±0.0005 | 0.03 | 0.0000 |
| INNER | 0.260 | 0.47 | -0.0039±0.0005 | 0.34 | 0.0000 |

1369

1370 Table 2: Seasonal amplitude of monthly pH means (SS_{range}) and long-term trends
 1371 ($t_{interannual}$) of pH in five regions and significant regression coefficients between the in
 1372 situ pH measurements and the monthly mean pH values (r^2_{ss}) and the regression
 1373 coefficient of the temporal variability of the deseasonalized pH measurements (r^2).

1374

1375

1376

1377

1378

1379

1380

1381

1382

1383

1384

1385

1386

1387

1388

1389

1390

1391

1392

1393

1394

1395

1396 Appendix A

1397

1398 Table A1: Vertical distribution of seasonal mean values and standard deviation (mean \pm

1399 standard deviation) of temperature, salinity, pH_T, oxygen and nitrate in the region South

1400 Ocean shown in Fig. 1.

| | z (m) | winter | spring | summer | autumn |
|---------------------------------------|----------|-------------------|-------------------|------------------|-------------------|
| temperature (°C) | 0-5 | 13.6 \pm 0.5 | 13.4 \pm 0.7 | 17.9 \pm 0.7 | 17.7 \pm 1.5 |
| | 5-25 | 13.8 \pm 0.7 | 13.6 \pm 0.6 | 17.1 \pm 0.7 | 17.2 \pm 1.5 |
| | 25-75 | 13.9 \pm 0.6 | 13.2 \pm 0.4 | 14.1 \pm 0.5 | 14.9 \pm 1.0 |
| | 75-125 | 13.7 \pm 0.6 | 13.0 \pm 0.5 | 12.8 \pm 0.3 | 13.2 \pm 0.4 |
| | 125-200 | 13.5 \pm 0.6 | 12.6 \pm 0.4 | 12.3 \pm 0.3 | 12.6 \pm 0.3 |
| | 200-400 | 12.6 \pm 0.3 | 11.9 \pm 0.3 | 11.6 \pm 0.3 | 11.9 \pm 0.3 |
| | 400-600 | 11.5 \pm 0.1 | 11.3 \pm 0.1 | 11.1 \pm 0.2 | 11.2 \pm 0.2 |
| | 600-900 | | | 11.4 \pm 0.1 | 11.4 \pm 0.2 |
| | 900-1300 | 11.2 \pm 0.1 | 11.1 \pm 0.2 | 10.9 \pm 0.3 | 11.0 \pm 0.3 |
| salinity | 0-5 | 35.82 \pm 0.06 | 35.72 \pm 0.11 | 35.62 \pm 0.07 | 35.71 \pm 0.08 |
| | 5-25 | 35.85 \pm 0.06 | 35.67 \pm 0.15 | 35.62 \pm 0.07 | 35.69 \pm 0.09 |
| | 25-75 | 35.85 \pm 0.05 | 35.74 \pm 0.09 | 35.71 \pm 0.06 | 35.76 \pm 0.08 |
| | 75-125 | 35.86 \pm 0.07 | 35.76 \pm 0.07 | 35.70 \pm 0.04 | 35.76 \pm 0.07 |
| | 125-200 | 35.80 \pm 0.10 | 35.73 \pm 0.06 | 35.64 \pm 0.04 | 35.72 \pm 0.06 |
| | 200-400 | 35.71 \pm 0.04 | 35.65 \pm 0.04 | 35.59 \pm 0.05 | 35.64 \pm 0.05 |
| | 400-600 | 35.64 \pm 0.04 | 35.65 \pm 0.05 | 35.64 \pm 0.05 | 35.64 \pm 0.03 |
| | 600-900 | | | 35.89 \pm 0.09 | 35.99 \pm 0.06 |
| | 900-1300 | 36.17 \pm 0.02 | 36.18 \pm 0.02 | 36.19 \pm 0.03 | 36.17 \pm 0.07 |
| pH _T | 0-5 | 8.10 \pm 0.02 | 8.12 \pm 0.02 | 8.11 \pm 0.02 | 8.09 \pm 0.02 |
| | 5-25 | 8.11 \pm 0.02 | 8.14 \pm 0.02 | 8.12 \pm 0.02 | 8.09 \pm 0.02 |
| | 25-75 | 8.11 \pm 0.01 | 8.12 \pm 0.01 | 8.11 \pm 0.02 | 8.08 \pm 0.02 |
| | 75-125 | 8.10 \pm 0.01 | 8.09 \pm 0.02 | 8.08 \pm 0.03 | 8.06 \pm 0.02 |
| | 125-200 | 8.07 \pm 0.03 | 8.07 \pm 0.03 | 8.06 \pm 0.03 | 8.05 \pm 0.02 |
| | 200-400 | 8.05 \pm 0.01 | 8.04 \pm 0.01 | 8.04 \pm 0.02 | 8.03 \pm 0.01 |
| | 400-600 | 8.02 \pm 0.01 | 8.017 \pm 0.002 | 8.02 \pm 0.02 | 8.01 \pm 0.01 |
| | 600-900 | | | 8.01 \pm 0.02 | 7.984 \pm 0.003 |
| | 900-1300 | 8.025 \pm 0.004 | 8.024 \pm 0.002 | 8.03 \pm 0.01 | 8.01 \pm 0.02 |
| oxygen (μ mol kg ⁻¹) | 0-5 | 249 \pm 6 | 265 \pm 17 | 250 \pm 12 | 244 \pm 12 |
| | 5-25 | 250 \pm 7 | 267 \pm 13 | 253 \pm 10 | 240 \pm 7 |
| | 25-75 | 249 \pm 8 | 255 \pm 9 | 247 \pm 7 | 236 \pm 8 |
| | 75-125 | 247 \pm 9 | 247 \pm 9 | 232 \pm 4 | 227 \pm 7 |
| | 125-200 | 230 \pm 11 | 237 \pm 9 | 226 \pm 6 | 224 \pm 6 |
| | 200-400 | 227 \pm 11 | 224 \pm 8 | 213 \pm 7 | 220 \pm 8 |
| | 400-600 | 209 \pm 6 | 205 \pm 5 | 196 \pm 7 | 200 \pm 4 |
| | 600-900 | | | 186 \pm 2 | 184 \pm 2 |
| | 900-1300 | 187 \pm 1 | 189 \pm 3 | 188 \pm 4 | 185 \pm 3 |

1401

1402

1403

1404

1405

1406

1407

1408

1409 Table A2: Monthly mean values and standard deviation (mean \pm standard deviation) of
 1410 temperature, salinity, pH_T, oxygen concentration, nitrate concentration and chlorophyll
 1411 at the surface waters for five geographical boxes shown in Fig. 1: South Ocean, RB
 1412 shelf and outer, middle and inner Ría de Vigo.

| | month | OCEAN | SHELF | OUTER | MIDDLE | INNER |
|------------------|-------|------------|------------|------------|------------|------------|
| temperature (°C) | Jan | 14.3±0.4 | 14.2±0.4 | 13.1±0.8 | 13.0±0.7 | 12.5±0.4 |
| | Feb | 13.3±0.2 | 13.1±0.6 | 13.0±0.7 | 12.7±0.7 | 12.6±0.7 |
| | Mar | 13.0±0.6 | 12.9±0.5 | 13.4±0.4 | 13.3±0.6 | 13.2±0.6 |
| | Apr | 14.1±0.4 | 14.0±0.3 | 14.8±1.2 | 14.0±0.9 | 14.4±1.1 |
| | May | 14.1±0.9 | 14.1±1.1 | 14.7±1.0 | 15.6±1.5 | 15.1±1.3 |
| | Jun | 17.5±1.1 | 16.1±0.9 | 17.1±1.0 | 17.3±1.3 | 18.4±1.1 |
| | Jul | 17.7±0.6 | 16.6±1.0 | 17.2±1.0 | 17.9±1.5 | 16.9±1.2 |
| | Aug | 17.7±0.9 | 16.7±0.6 | 16.0±1.7 | 17.5±1.5 | 16.8±1.7 |
| | Sep | 18.5±1.3 | 16.5±1.3 | 17.3±1.3 | 17.1±1.2 | 17.8±1.4 |
| | Oct | 17.9±0.4 | 17.0±0.6 | 16.6±0.9 | 15.4±1.1 | 15.8±1.0 |
| | Nov | 15.6±0.6 | 15.3±1.1 | 15.6±1.4 | 15.2±0.9 | 14.9±1.2 |
| | Dec | 15.1±0.3 | 14.8±0.2 | 14.8±1.3 | 14.1±0.9 | 14.6±1.1 |
| salinity | Jan | 35.88±0.13 | 35.77±0.18 | 33.92±0.82 | 33.57±2.37 | 34.26±1.44 |
| | Feb | 35.81±0.04 | 35.37±0.84 | 34.33±1.63 | 33.30±2.51 | 30.86±4.78 |
| | Mar | 35.81±0.04 | 35.24±0.71 | 34.43±0.77 | 34.52±1.12 | 34.42±1.25 |
| | Apr | 35.72±0.07 | 35.43±0.47 | 35.24±0.29 | 34.58±0.90 | 34.72±0.74 |
| | May | 35.59±0.12 | 35.45±0.25 | 34.47±1.37 | 34.38±1.09 | 33.99±2.29 |
| | Jun | 35.64±0.13 | 35.56±0.12 | 34.62±0.81 | 34.87±0.74 | 34.42±0.54 |
| | Jul | 35.60±0.07 | 35.58±0.08 | 35.36±0.26 | 35.27±0.38 | 35.19±0.50 |
| | Aug | 35.57±0.05 | 35.59±0.05 | 35.48±0.22 | 35.45±0.21 | 35.37±0.17 |
| | Sep | 35.72±0.12 | 35.48±0.18 | 35.33±0.19 | 35.32±0.29 | 35.20±0.27 |
| | Oct | 35.74±0.05 | 35.65±0.10 | 34.94±0.56 | 34.84±0.88 | 33.98±1.45 |
| | Nov | 35.81±0.06 | 35.67±0.11 | 34.85±0.77 | 34.23±0.85 | 33.73±2.80 |
| | Dec | 35.85±0.06 | 35.89±0.26 | 33.76±1.36 | 33.77±1.51 | 27.95±5.50 |
| pH _T | Jan | 8.09±0.03 | 8.08±0.03 | 8.12±0.06 | 8.05±0.05 | 8.02±0.04 |
| | Feb | 8.09±0.02 | 8.10±0.03 | 8.11±0.05 | 8.07±0.05 | 8.05±0.06 |
| | Mar | 8.11±0.01 | 8.11±0.03 | 8.18±0.08 | 8.13±0.07 | 8.18±0.08 |
| | Apr | 8.11±0.02 | 8.13±0.03 | 8.16±0.05 | 8.13±0.05 | 8.11±0.07 |
| | May | 8.12±0.02 | 8.14±0.04 | 8.19±0.04 | 8.13±0.08 | 8.11±0.07 |
| | Jun | 8.08±0.03 | 8.13±0.03 | 8.15±0.04 | 8.10±0.07 | 8.04±0.09 |
| | Jul | 8.11±0.02 | 8.13±0.02 | 8.11±0.06 | 8.09±0.07 | 8.02±0.07 |
| | Aug | 8.09±0.03 | 8.11±0.03 | 8.11±0.07 | 8.07±0.09 | 7.92±0.05 |
| | Sep | 8.09±0.02 | 8.11±0.03 | 8.09±0.05 | 8.03±0.07 | 7.98±0.11 |
| | Oct | 8.09±0.01 | 8.11±0.03 | 8.06±0.06 | 8.00±0.08 | 7.94±0.09 |
| | Nov | 8.11±0.02 | 8.09±0.02 | 8.09±0.07 | 8.00±0.06 | 7.90±0.12 |
| | Dec | 8.11±0.01 | 8.12±0.01 | 8.06±0.03 | 8.02±0.04 | 7.98±0.02 |

1413

1414
 1415
 1416
 1417
 1418
 1419

Table A2: Continued

| | month | OCEAN | SHELF | OUTER | MIDDLE | INNER |
|-------------------------------------|-------|-----------|---------|---------|---------|---------|
| oxygen ($\mu\text{mol kg}^{-1}$) | Jan | 244±6 | 246±5 | 265±8 | 252±16 | 242±11 |
| | Feb | 255±5 | 259±12 | 255±13 | 254±15 | 252±14 |
| | Mar | 258±16 | 268±19 | 280±27 | 276±23 | 260±28 |
| | Apr | 268±5 | 270±7 | 271±13 | 276±25 | 249±26 |
| | May | 271±13 | 269±14 | 286±22 | 287±25 | 260±12 |
| | Jun | 244±3 | 266±11 | 270±17 | 284±26 | 232±19 |
| | Jul | 247±12 | 263±11 | 269±23 | 271±25 | 234±23 |
| | Aug | 247±9 | 259±8 | 265±23 | 277±27 | 204±21 |
| | Sep | 241±9 | 261±14 | 272±18 | 251±26 | 228±34 |
| | Oct | 259±13 | 250±12 | 249±20 | 226±21 | 215±16 |
| | Nov | 243±11 | 242±4 | 236±9 | 230±16 | 209±26 |
| | Dec | 243±10 | 240±12 | 248±11 | 237±14 | 242±16 |
| nitrate ($\mu\text{mol kg}^{-1}$) | Jan | 2.3±0.5 | 2.7±0.8 | 5.3±2.6 | 7.1±3.8 | 7.6±2.0 |
| | Feb | 3.4±0.7 | 5.0±2.6 | 6.3±3.0 | 6.3±3.4 | 8.6±4.5 |
| | Mar | 4.9±2.4 | 3.5±2.9 | 2.1±2.5 | 2.0±2.4 | 4.5±2.3 |
| | Apr | 0.1±2.4 | 0.4±0.7 | 0.4±0.5 | 0.8±1.0 | 0.6±0.6 |
| | May | 0.02±0.03 | 0.6±0.4 | 0.5±0.4 | 0.5±0.8 | 0.7±1.3 |
| | Jun | 0.04±0.02 | 0.1±0.1 | 0.1±0.3 | 0.3±0.4 | 0.8±0.8 |
| | Jul | 0.1±0.1 | 0.0±0.1 | 0.3±0.6 | 0.5±0.7 | 1.1±0.8 |
| | Aug | 0.08±0.03 | 0.1±0.1 | 1.1±1.6 | 0.6±0.9 | 3.3±3.2 |
| | Sep | 0.1±0.1 | 0.2±0.7 | 1.0±0.9 | 0.9±1.1 | 2.1±1.4 |
| | Oct | 1.7±0.8 | 0.3±0.7 | 2.2±2.4 | 3.4±2.7 | 3.1±1.5 |
| | Nov | 0.1±0.1 | 1.2±2.9 | 3.8±2.9 | 4.3±2.3 | 7.2±3.2 |
| | Dec | 0.4±0.9 | 1.3±1.0 | 6.0±3.1 | 5.7±2.7 | 8.2±4.1 |
| chlorophyll (mg m^{-3}) | Jan | 0.5±0.1 | 0.6±0.1 | 0.9±0.2 | 1.0±0.9 | 0.9±0.3 |
| | Feb | 0.5±0.1 | 0.8±0.3 | 2.3±1.5 | 1.8±1.6 | 1.3±0.9 |
| | Mar | 0.5±0.2 | 1.4±1.5 | 3.7±2.8 | 3.9±3.2 | 3.5±2.3 |
| | Apr | 2.6±1.1 | 1.8±1.4 | 3.0±1.8 | 4.2±2.4 | 3.7±2.1 |
| | May | 0.5±0.2 | 0.6±0.6 | 4.1±3.0 | 4.5±4.5 | 3.4±2.6 |
| | Jun | 0.8±0.8 | 0.7±0.6 | 3.8±1.7 | 4.4±2.7 | 5.2±3.2 |
| | Jul | 0.4±0.2 | 0.7±0.7 | 3.2±1.9 | 4.4±2.5 | 5.0±2.2 |
| | Aug | 0.5±0.2 | 0.8±0.5 | 2.7±2.3 | 5.5±4.1 | 2.0±2.3 |
| | Sep | 0.5±0.3 | 1.6±1.0 | 4.3±2.4 | 5.8±3.6 | 5.1±3.7 |
| | Oct | 0.3±0.1 | 0.8±0.5 | 4.6±4.1 | 3.3±3.5 | 2.7±1.9 |
| | Nov | 0.8±0.3 | 0.9±0.8 | 2.4±1.1 | 1.7±2.4 | 1.6±1.0 |
| | Dec | 0.5±0.2 | 0.4±0.6 | 1.5±0.8 | 1.0±0.6 | 1.2±0.3 |

1420
 1421
 1422
 1423
 1424